Deep impact of the inactivation of the SecA2-only protein export pathway on the proteosurfaceome of Listeria monocytogenes

Ingrid Chafsey, Rafal Ostrowski, Morgan Guilbaud, Pilar Teixeira, Jean-Marie Herry, Nelly Caccia, Christophe Chambon, Michel Hébraud, Joana Azeredo, Marie-Noëlle Bellon-Fontaine, et al.

Deep impact of the inactivation of the SecA2-only protein export pathway on the proteosurfaceome of *Listeria monocytogenes*

Ingrid CHAFSEY [#], Rafal OSTROWSKI [#], Morgan GUILBAUD, Pilar TEIXEIRA, Jean-Marie HERRY, Nelly CACCIA, Christophe CHAMBON, Michel HÉBRAUD, Joana AZEREDO, Marie-Noëlle BELLON-FONTAINE, Magdalena POPOWSKA* and Mickaël DESVAUX*

GRAPHICAL ABSTRACT

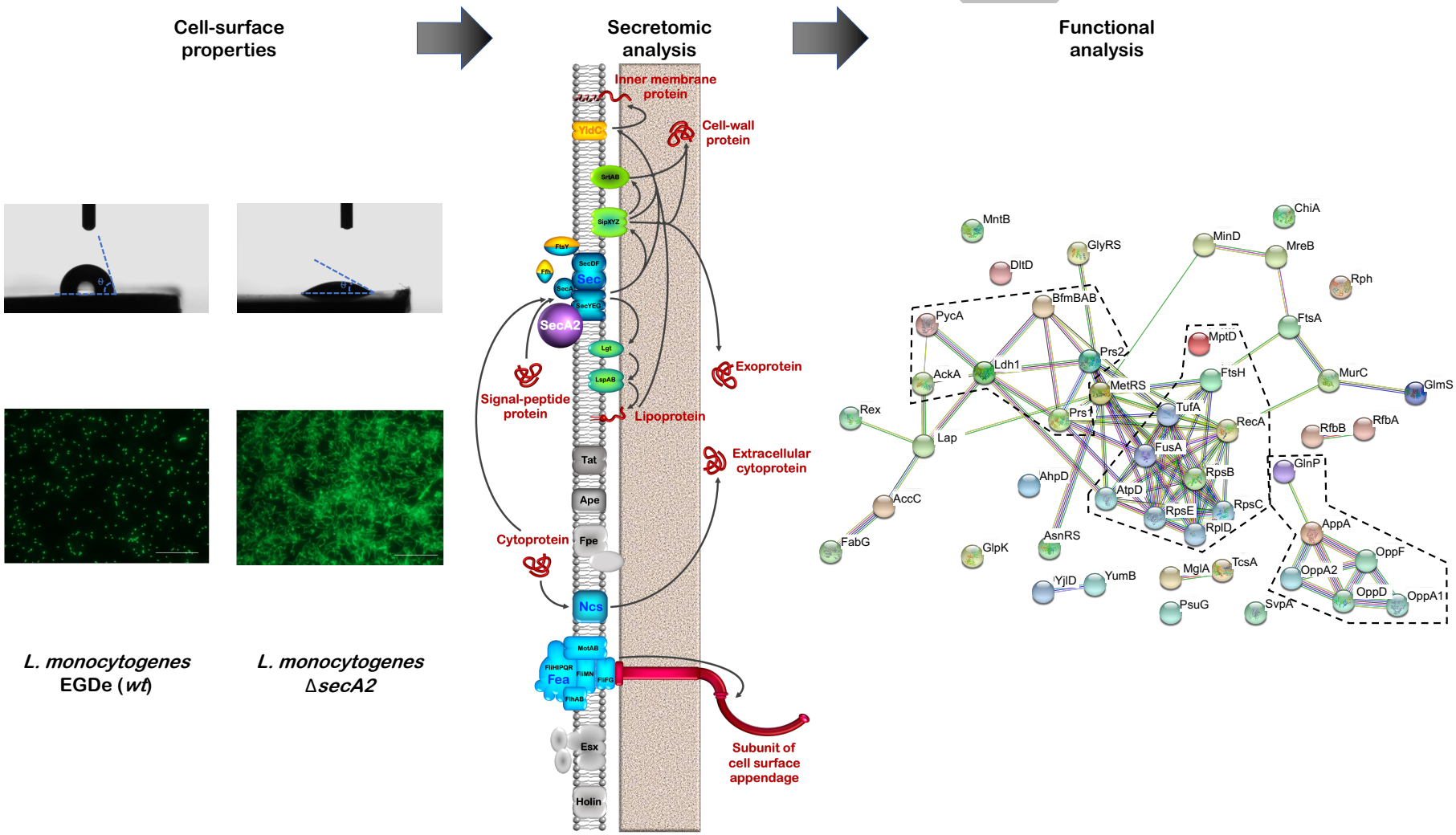

L. monocytogenes EGDe (*wt*)

L. monocytogenes Δ*secA2*

Deep impact of the inactivation of the SecA2-only protein export pathway on the proteosurfaceome of *Listeria monocytogenes*

Ingrid CHAFSEY [1,#], Rafal OSTROWSKI [2,#], Morgan GUILBAUD [3], Pilar TEIXEIRA [4], Jean-Marie HERRY [3], Nelly CACCIA [1], Christophe CHAMBON [5], Michel HÉBRAUD [1,5], Joana AZEREDO [4], Marie-Noëlle BELLON-FONTAINE [3], Magdalena POPOWSKA [2,*] and Mickaël DESVAUX [1,*]

[1] INRAE, Université Clermont Auvergne, UMR454 MEDiS, 63000 Clermont-Ferrand, France

[2] University of Warsaw, Faculty of Biology, Department of Bacterial Physiology, Applied Microbiology, Institute of Microbiology, Warsaw, Poland

[3] Université Paris-Saclay, INRAE, AgroParisTech, UMR SayFood, 91300 Massy, France

[4] University of Minho, Centre of Biological Engineering, Campus de Gualtar, Braga, 4710-057, Portugal

[5] INRAE, Plateforme d'Exploration du Métabolisme, 63122 Saint-Genès Champanelle, France

[#] These authors contributed equally to this work and thus share first authorship

*Correspondence: Dr Hab Magdalena POPOWSKA, University of Warsaw, Faculty of Biology, Department of Bacterial Physiology, Institute of Microbiology, Miecznikowa 1, 02-096, Warsaw, Poland. Tel.: +48 22 55 41 420, Fax: +48 22 55 41 402, E-mail: magdapop@biol.uw.edu.pl

Dr Hab Mickaël DESVAUX-LENÔTRE, INRAE (Institut National de Recherche pour l'Agriculture, l'Alimentation et l'Environnement) Clermont-Auvergne-Rhône-Alpes, UMR454 MEDiS (Microbiologie, Environnement Digestif, Santé), Site de Theix, F-63122 Saint-Genès Champanelle, France. Tel.: +33 (0)4 73 62 47 23, Fax: +33 (0)4 73 62 45 81, E-mail: mickael.desvaux@inrae.fr

ABSTRACT

L. monocytogenes presents a dimorphism associated to the SecA2 activity with cells having a normal rod shape or a dysmorphic elongated filamentous form. Besides variation of the cell and colony morphotype, this cell differentiation has profound ecophysiological and physiopathological implications with collateral effects on virulence and pathogenicity, biotope colonisation, bacterial adhesion and biofilm formation. This suggests the SecA2-only protein export could influence the listerial cell surface, which was investigated first by characterising its properties in *L. monocytogenes wt* and Δ*secA2*. The degree of hydrophilicity and Lewis acid-base properties appeared significantly affected upon SecA2 inactivation. As modification of electrostatic properties would owe to modification in the composition of cell-surface proteins, the proteosurfaceome was further investigated by shotgun label-free proteomic analysis with a comparative relative quantitative approach. Following secretomic analysis, the protein secretion routes of the identified proteins were mapped considering the cognate transport and post-translocational maturation systems, as well as protein categories and subcellular localisation. Differential protein abundance profiles coupled to network analysis revealed the SecA2 dependence of 48 proteins, including some related to cell envelope biogenesis, translation and protein export, which could account for modifications of adhesion and cell properties of *L. monocytogenes* upon SecA2 inactivation. This investigation unravelled the profound influence of SecA2 activity on the cell surface properties and proteosurfaceome of *L. monocytogenes*, which provides advanced insights about its ecophysiopathology.

Keywords: SecA2-export pathway ; bacterial secretion systems ; cell surface properties ; cell surface proteome ; secretomic analysis

INTRODUCTION

Listeria monocytogenes is a foodborne zoonotic pathogen and etiological agent of human listeriosis, which invasive forms exhibit the most severe clinical symptoms, namely febrile gastroenteritis, septicaemia, encephalitis, meningitis or late spontaneous abortions [1,2]. This disease is rare with a low incidence, varying worldwide between 0.1 and 11.3 cases per million population per year, but with a high mortality rate generally ranging around 20-30 % [3,4]. Listeriosis primarily affects population at risk with a weakened immune system, essentially pregnant women, infants, and elderly [5]. *L. monocytogenes* is a ubiquitous bacterium, it is widespread in reared animals, telluric and hydric environment where it lives as a saprophyte. *L. monocytogenes* is able to tolerate, survive and/or multiply over a wide range of environmental conditions [6], *e.g.* low water activity, relatively high salt concentrations, successive freezing-thawing, over long periods of drought or wide pH and temperatures. While its ability to form biofilm has sometimes been questioned and doubted by some authors, it is now clearly recognised and established this species is enabled to colonise surfaces, which participate to its ability to persist in agrifood environments and all along the food chain, from the natural environments, animals, food matrices and food processing, ultimately causing human infection [7–11]. Whenever for the cell infection, adaptive cell response or surface colonisation, the listerial cell surface is the interface requires and enabling bacterial cells to interacts with their surroundings.

The cell-envelope proteins play a key role in such interactions [12,13]. In parietal monoderm bacteria (archetypal Gram-positive bacteria) proteins have to cross the cytoplasmic membrane (CM; GO:0005886) *via* protein export pathways to reach their final subcellular location (SCL) to the cell envelope. In *L. monocytogenes*, seven protein export systems have been uncovered to date where the Sec (secretion) pathway appears as the major trafficking route, with an estimated number of 714 proteins [14–18]. Upon translocation, these Sec-secreted proteins exhibiting a N-terminal signal peptide (SP) can have different final destinations within the cell-envelope of CW-monoderm bacterial

74 cell, namely either at the CM or cell wall (CW). In line with the gene ontology (GO) for cellular
75 component [19], some proteins can be localised intrinsically at the CM (GO:0031226), either integral
76 to the CM (iCM; GO:0005887), *i.e.* integral membrane proteins (IMPs) embedded to the CM *via*
77 transmembrane hydrophobic α-helical domain (TMD), or anchored to the CM (aCM; GO:0046658),
78 namely lipoproteins tethered to the CM by a lipid moiety [12]; as predicted through majority vote,
79 *L. monocytogenes* EGDe encodes 524 IMPs with a SP, either of type I (SP1), type II (SP2) or
80 uncleaved (uSP), and 74 lipoproteins with a SP2 [14]. At the CW (GO:0009275), proteins can be
81 either anchored covalently to the peptidoglycan by sortases *via* their C-terminal LPXTG domain, *i.e.*
82 43 LPXTG-proteins in *L. monocytogenes* EGDe, or attached non-covalently through CW-binding
83 motifs, namely 4 WXL-proteins, 3 LysM-proteins, 1 PGBD1-protein and 5 proteins with SH3-8
84 (previously known as GW) domains [13,14]. While additional proteins predicted as localised at the
85 cell surface (GO:0009986) include cell-surface supramolecular structures, namely flagella and
86 putative pseudo-pili, respectively secreted and assembled *via* the flagellum export apparatus (Fea)
87 and fimbrilin-protein exporter (Fpe), about 80 % of cell-envelope proteins of *L. monocytogenes*
88 EGDe thus appear as secreted in a Sec-dependent manner [14].

89 Beside a SP, export across the SecYEG protein conducting-channel (translocon) necessitates
90 energy provided by the essential peripheral ATPase SecA, which together form the translocase
91 [20,21]. In all mycolate-diderm bacteria (archetypical acid-fast bacteria, namely mycobacteria) but
92 just in a couple of pathogenic CW-monoderm bacteria, including *L. monocytogenes*, a truncated and
93 accessory paralogue of SecA has been identified and named SecA2 [22]. The SecA2-only protein
94 export pathway (by contrast to system where SecA2 is accompanied with a duplication of SecY)
95 assists and improves the secretion efficiency through the Sec translocase [23,24]. In
96 *L. monocytogenes,* the SecA2-only pathway was shown to enable secretion of specific proteins,
97 including MurA [muramidase A, formerly called NamA (N-acetylmuramidase A)] and CwhA [cell
98 wall hydrolase A, formerly called P60 (protein of 60 kDa) or Iap (Invasion associated protein)] [25–

99 28]. Decrease secretion of these CW hydrolases upon SecA2 inactivation results in septation defect
100 leading to elongated cells, which results in bacterial cell dysmorphism with collateral effects on the
101 colony morphology [27,29], surface colonisation and biofilm architecture [30,31], as well as
102 virulence level of *L. monocytogenes* [26,32]. This dimorphism of *L. monocytogenes*, between rod and
103 filamentous cell shapes, has been early reported, from clinical, food and environmental isolates
104 [30,33–36] but the molecular regulatory mechanism of SecA2 in the morphotype conversion remain
105 unclear [30,31,37].

106 Most recent exoproteomic analysis allowed the identification of additional SecA2-dependent
107 exoproteins associated to CW metabolism, *e.g.* peptidoglycan lytic P45 (protein of 45 kDa) or
108 muralytic transglycosylase SpsB (stationary phase survival protein B), which exhibit a SP1, like
109 NamA and CwhA, but the specific molecular determinant addressing these proteins to the SecA2-
110 only export pathway remains undetermined [38]. As such, proteins secreted in a SecA2-dependent
111 manner cannot be predicted by proteogenomic analysis [14] and this is further challenged by an
112 additional peculiar feature lying in the ability of the SecA2-only pathway to secrete several specific
113 exoproteins with no N-terminal SP [26,38], *e.g.* Sod (superoxide dismutase) [39], Lap (*Listeria*
114 adhesion protein) [40], GAPDH (glyceraldehyde 3-phosphate dehydrogenase, Gap), or DnaK [38].
115 Together with Lap, which is a bifunctional alcohol/acetaldehyde dehydrogenase, Gap and DnaK are
116 primarily cytoplasmic proteins that moonlight when located extracellularly and are involved in
117 bacterial adhesion [41,42]. As suggested by mislocation of key cell-surface virulence factors InlA
118 and ActA upon abnormal cell division in CwhA mutant [43], differential autolytic activities of
119 bacterial cell-surface fraction [26] and biofilm formation ability in SecA2 mutant [31], the SecA2-
120 only protein export could influence the listerial cell surface but this aspect has never been investigated
121 further so far. By characterising first, the bacterial cell surface properties of *L. monocytogenes*
122 expressing or inactivated in the SecA2 pathway, the degree of hydrophilicity and Lewis acid-base
123 properties appeared to be significantly affected. As modification of electrostatic properties would

owe to modification in the composition of cell-surface proteins, this prompted us to investigate further the proteinaceous subset of the surfaceome, *i.e.* the proteosurfaceome, of *L. monocytogenes* by a comparative relative quantitative approach, which appeared as quite impacted upon SecA2 inactivation.

MATERIAL & METHODS

Bacterial strains and culture conditions

L. monocytogenes EGDe wild type (*wt*) strain [44] and the isogenic mutant strain deleted of *secA2* [38] were grown in brain-heart infusion (BHI) broth. As previously described [38], each bacterial strain from a -80°C cryotube were plated on BHI agar and incubated at 37 °C. A preculture was set up from one isolated bacterial colony and grown in BHI broth at 37°C under orbital shaking (150 rpm). Cells were then inoculated at an $OD_{600\ nm}$ of 0.01 in BHI broth in the same conditions as preculture and grown until late exponential phase.

Bacterial cell surface properties

Direct electrophoretic mobility measurements were performed in order to obtain the surface charge characteristics of *L. monocytogenes* EGDe *wt* and isogenic mutant strains [45,46]. In brief and as previously described [47], bacterial cells were grown overnight, centrifuged (7000 *g,* 10 min), and the cells were washed twice and resuspended in 1.5 mM NaCl. The pH of each suspension was adjusted from 5.6 (corresponding to starting pH) to 2 by addition of HNO_3 solution. Electrophoretic mobility measurements were taken at room temperature in a 50 V electric field using a Laser Zetameter (CAD Instrumentation, Les Essarts le Roi, France). For each measurement, results were based on the automated video analysis of about 200 bacterial cells. Each experiment was performed in duplicate (technical repeats) on three independent cultures (biological replicates).

The measurements of contact angles were made on *L. monocytogenes* cell lawns on membrane filters [48]. Briefly and as previously described [49], a suspension of bacterial cells, adjusted to a concentration of approximately 1.10^9 cells.ml^{-1} in saline solution (150 mM NaCl), was deposited onto

149 a 0.45 µm cellulose filter, previously wetted with distilled water. To standardise the moisture content,
150 the filters with the resultant lawn of cells deposited were then left to dry on Petri dishes containing
151 1 % (w/v) agar and 10 % (v/v) glycerol. Contact angles were measured by the sessile drop technique
152 on the cell lawns, using a contact angle measurement apparatus (CA 15 Plus, Dataphysics). The
153 degree of hydrophobicity (ΔG_{1w1}) was evaluated through contact angle measurements [50,51].
154 Besides qualitative assessment of the hydrophobicity, it was possible to determine the absolute degree
155 of hydrophobicity (ΔG_{1w1}) of any substance vis-à-vis water (w), which can be precisely expressed in
156 applicable S.I. units [46,50]; the measurements were made at room temperature, using three different
157 liquids, *i.e.* water, formamide and 1-bromonaphtalene. At least 25 measurements for each liquid and
158 bacterial strain were performed at room temperature and allowed calculation of the surface tension
159 components, namely the apolar Lifshtz-van der Waals surface energy component (γ_S^{LW}), electron
160 acceptor surface energy component (γ_S^{+}), electron donator surface free energy component (γ_S^{-}), polar
161 Lewis acid-base component (γ_S^{AB}), and total surface free energy (γ_S^{T}).

162 To complete contact angle measurements, hydrophobic/hydrophilic properties of bacterial
163 cells were evaluated using MATS (microbial affinity to solvents) method as previously developed
164 and methodically described [52]. In brief, cell suspensions were prepared in saline solution (150 mM
165 NaCl) and placed into a glass test tube with different solvents, *i.e.* either chloroform ($CHCl_3$),
166 hexadecane ($C_{16}H_{34}$), decane ($C_{10}H_{22}$) or ethyl acetate ($C_4H_{10}O$). In each case, the $OD_{400\ nm}$ were
167 measured for the aqueous phases before and after vortexing and decantation. The affinity of the
168 bacterial cells for the solvent phase is calculated as the proportion of the cells (in percentage) that
169 were excluded from the aqueous phase.

170 **Bacterial adhesion assay**

171 Bacterial adhesion assays were performed in static conditions as previously described [53].
172 Briefly, after centrifugation of bacterial cell cultures (7000 *g*, 10 min), cell pellets were washed three
173 times in 150 mM NaCl by centrifugation and their concentrations were adjusted to 10^7 CFU.mL^{-1}.

174 The material coupons, namely stainless steel 316 (Goodfellow, UK), PET (Goodfellow, UK) and
175 glass (Gerhard Menzel GmbH, Germany), were immersed in the cell suspensions for 3 h at 37°C.
176 Each material coupon was then rinsed five times in 150 mM NaCl to remove non- or weakly-attached
177 bacterial cells. For direct observations of bacterial cells, fluorescent labelling was performed for
178 15 min in the dark by immersing each material in distilled water containing SYTO9 at 1 µM
179 (Invitrogen, ThermoFisher). Epifluorescence microscopic observations were performed with an
180 objective ×40 (Leica Microsystems, Nanterre, France) and results expressed as the number of
181 adhering bacterial cells per cm². Of note, bacterial cells for *L. monocytogenes* Δ*secA2* are elongated
182 and approximately 10 times longer than the *wt* [27,31]. Each experiment was performed from two
183 independent cultures.

184 **Isolation of bacterial cell-surface proteins**

185 Bacterial cell-surface proteins were isolated following biotinylation and protein affinity
186 purification using sulfo-NHS-SS-biotin (sulfosuccinimidyl 2-(biotinamido)-ethyl-1-3'-
187 dithiopropionate) for protein labelling and neutravidin for purification [54–56]. Cells were harvested
188 by centrifugation (4000 *g*, 5 min) at room temperature (RT) and then washed three times in 10 mM
189 PBS pH 8 supplemented with 1 mM phenylmethanesulfonyl fluoride (PMSF). After centrifugation,
190 pelleted cells were weighed to ensure the same amount of wet cells (100 mg) and then labelled with
191 sulfo-NHS-SS-biotin (1.5 mM) for 1 min at RT. After quenching the excess of biotinylation reagent
192 with glycine buffer (500 mM in PBS as above) and centrifugation (three times), cells were
193 resuspended in lysis buffer (1 % Triton X-100 and 1 mM PMSF in PBS as above). Cells were
194 disrupted with glass microbeads using FastPrep-24 classic (MP Biomedicals) with two steps of 20 s
195 at 6 m/s, cell debris discarded by centrifugation (20 000 *g*, 30 min, 4°C) and exactly the same volume
196 of each biotinylated protein samples was loaded for affinity purification using neutravidin agarose
197 resin (Pierce Thermo Scientific, 400 µl). After washing with ten column volumes (10 mM PBS, pH 8,
198 1 % NP-40), labelled proteins were specifically eluted by cleaving sulfo-NHS-SS-biotin disulfide

199 bond (2 % SDS, 20 % glycerol, 5 % β-mercaptoethanol, 50 mM dithiothreitol, 62.5 mM Tris-HCl,
200 pH 6.8).

201 **Protein preparation for LC-MS/MS analysis**

202 To eliminate interfering molecules (such as salts) and concentrate proteins in a single band of
203 polyacrylamide gel, each sample was submitted to a short SDS-PAGE (sodium dodecyl sulfate–
204 polyacrylamide gel electrophoresis) migration in a BioRad Mini Protean II unit with a stacking gel at
205 4 % (pH 6.8) and resolving gel at 12.5 % (pH 8.8) using acrylamide/bisacrylamide (29/1 ratio). To
206 avoid bias in the comparison of protein abundance by relative quantification analyses, labelled
207 proteins were adjusted respective to the same amount of biomass between the wild strain and the
208 isogenic mutant strain deleted of *secA2*. After the addition of the same volume of Laemmli buffer
209 (2 % SDS, 25 % glycerol, 5 % β-mercaptoethanol, 0.005 % bromphenol blue and 62.5 mM Tris-HCl,
210 final) and heating at 95°C for 5 min, exactly the same volume of protein extracts was migrated and
211 just allowed to penetrate in the first few millimetres of the resolving gel after a few minutes migration
212 (15 mA/gel). Gel was then stained with Coomassie Brilliant Blue G250 [57,58] and the single bands
213 in each lane were excised. First, the gel bands were destained in 25 mM ammonium bicarbonate with
214 acetonitrile (5 %) for 30 min and twice in 25 mM ammonium bicarbonate with acetonitrile (50 %)
215 for 30 min. Second, the proteins in the gel were reduced in 100 mM ammonium bicarbonate with
216 10 mM dithiothreitol for 60 min at 55°C, and alkylated with 55 mM iodoacetamide for 20 min at RT
217 in the dark. The gel bands were washed once in 25 mM ammonium bicarbonate in 5 % acetonitrile
218 for 30 min and twice in 25 mM ammonium bicarbonate in 50 % acetonitrile for 30 min each. The gel
219 bands were dehydrated with 100 % acetonitrile, then the samples were hydrolysed with 600 ng of
220 trypsin (Promega) for 5 h at 37°C and the peptides extracted with 100 % acetonitrile. After air drying,
221 the hydrolysed samples were resuspended in the same volume of a acetonitrile (5 %) and formic acid
222 (0.1%) aqueous solution before injection (8 µl) and nanoHPLC separation (Ultimate 3000, Dionex)
223 with a pre-column (LC-Acclaim PepMap100 C18, ThermoScientific, 5 mm length by 100 µm, 100 Å

224 nanoViper, 5 µm) followed by an analytical column (LC-Acclaim PepMap100 C18,
225 ThermoScientific, 25 cm length by 75 µm, 100 Å nanoViper, 3 µm,) with a gradient of an aqueous
226 acetonitrile solution (80 % acetonitrile, 0.5 % formic acid) from 0 to 60 % during 50 min. The
227 peptides separated on the nanoHPLC column were nanoelectrosprayed *via* a nanoCaptiveSpray
228 source (Bruker) in a QTOF mass spectrometer (IMPACTII, Bruker) in mode CID (ProteinID-
229 InstantExpert_IBOn.m-profile), where each MS analysis is followed by a maximum of MS/MS
230 analyses for 3 seconds. Each condition was performed in triplicates (biological replicates) with two
231 runs per sample (technical repeats).

232 **Data processing and bioinformatic analysis**

233 For protein identification, Progenesis QI for Proteomics (QIP) was used *via* MASCOT v2.3
234 using a previously described home database corresponding to predicted mature proteins in *L.*
235 *monocytogenes* EGD-e [16]. Peptides were validated for a Mascot score permitting to obtain a false
236 discovery rate (FDR) at below 1 % and proteins were identified when at least two peptides matched
237 significantly (score higher than 20) in the database with search parameters set to 10 ppm for peptide
238 and 0.5 Da for fragment mass tolerance. FDR approach was applied to overcome the issue of multiple
239 hypothesis testing and *q*-values (adjusted *p*-values) were further calculated. Comparison of protein
240 abundance was performed following the standard workflow provided by Progenesis QIP for
241 proteomics applying the label-free relative quantification method using Hi-N mode (Nonlinear
242 Dynamics, Waters); basically, the MS1 survey scans are used for ion abundance quantification where
243 peptide ions falling within the robust estimation limits are used to calculate the normalisation factor
244 and selected as normalisation reference to compare peptidic signals between runs. Differential protein
245 quantification was considered significant for fold abundance greater than 1.5 and *p*-value lower than
246 0.05.

247 Secretomic analysis in *L. monocytogenes* was performed as previsouly described in details to
248 predict protein transport and post-translocational maturation pathways, protein categories and

249 subcellular localisations [14]. Network analysis to identify protein-protein links was performed using
250 STRING v11.0 as well as enrichment of gene ontology (GO) terms for molecular function further
251 analysed using Panther [59,60]; network clustering was performed using Markov chain cluster
252 algorithm (MCL) with an inflation parameter of 3.

253 **RESULTS**

254 **SecA2 inactivation impact bacterial cell surface properties of *L. monocytogenes* EGDe**

255 Considering that hydrophobic bacterial cells would tend to repeal water and aggregate
256 contrary to hydrophilic bacteria [61], the possible modification of cell surface properties upon
257 inactivation of SecA2 in *L. monocytogenes* EGDe was considered and assayed using an array of
258 complementary approaches. Assessing the bacterial cell surface charge using microelectrophoresis,
259 it first appears that both strains follow a parallel trend over pH variations (Figure 1A). Of note, global
260 net surface charges are more variable for *L. monocytogenes* Δ*secA2* cells as compared to *wt*
261 (Figure 1A), which could result from the different cell sizes between the *wt* and mutant. However, no
262 significant difference was apparent in their electronegative net surface charge. As reflected by
263 decreasing electrophoretic measurements, the maximum of electronegativity is found between pH 3
264 and 3.5. No isoelectric point was displayed by either strain confirming their marked Lewis acid-base
265 character.

266 As inferred qualitatively by the water contact angles (with θ_W below 65º), both
267 *L. monocytogenes wt* and Δ*secA2* strains were hydrophilic bacterial cells (Table 1). This is further
268 supported thermodynamically with positive values for the free energy of interaction among the
269 bacterial cells when immersed in water (ΔG_{1w1}) indicating cells are mostly hydrophilic (Table 1).
270 While surface tension components were in the same range for both strains, a slight change in the
271 surface hydrophilicity of *L. monocytogenes* upon SecA2 inactivation was observed as indicated by
272 variation of θ_W and ΔG_{1w1} between *L. monocytogenes* Δ*secA2* compared the *wt* strain. Further
273 analyses using MATS confirmed these results. As shown in Figure 1B, both listerial strains display

274 much higher affinity for chloroform, an electron accepting solvent with negligible donor feature, than
275 for apolar solvents (hexadecane or decane), and even less for ethyl acetate, a strongly electron donor
276 solvent. This indicates that polar interaction forces between bacterial surfaces and solvents resulted
277 from their strong electron donor character and weak electron acceptor character. While these results
278 first demonstrated that both bacterial cell surfaces were hydrophilic, it further confirmed bacterial
279 cell surface of *L. monocytogenes* was more hydrophilic upon SecA2 inactivation.

280 Investigating bacterial adhesion to different supports, it appeared *L. monocytogenes wt*
281 adhered similarly to stainless steel, glass and PET, while the adhesion of *L. monocytogenes* Δ*secA2*
282 cells appeared substratum-dependent (Figure 2). While microscopic observations confirmed
283 significant cell elongation of *L. monocytogenes* Δ*secA2* compared *wt* (Figure 2A), the increase of the
284 hydrophilic character of the Δ*secA2* mutant as compared to the *wt* was associated with a decrease in
285 the number of adhering cells (Figure 2B). Surprisingly, the number of adhering *L. monocytogenes*
286 Δ*secA2* cells (exhibiting hydrophilic properties) was lowest on the hydrophilic material, *i.e.* glass
287 (Figure 2B); this observation could result from the combination of the low interactions between
288 bacteria and glass surface and the size of the *L. monocytogenes* Δ*secA2* cells, promoting their
289 detachment from materials over rinsing. Altogether, these data strongly support the view that the
290 inactivation of SecA2 influences the bacterial cell surface properties by increasing the degree of
291 hydrophilicity, as well as impacting the Lewis acid-base properties, which could be due, at least in
292 part, to its electrostatic properties owing to modification in the composition of cell-surface proteins.

293 **Mapping the protein secretion routes by secretomic analysis of the proteosurfaceome in**
294 ***L. monocytogenes* EGDe**

295 In order to investigate the proteosurfaceome, biotin labelling of cell-surface proteins was
296 performed in *L. monocytogenes wt* and Δ*secA2* strains where a total of 116 distinct proteins were
297 identified by shotgun proteomics (supplementary material Table S1); none of them corresponded to
298 identical paralogues encoded in *L. monocytogenes* genome (*e.g.* UPI0000054D93 with Lmo0174,

299 Lmo0329 and Lmo0827) and were therefore proteins encoded by unique CDS. Prior to this proteomic
300 investigation, evidence of their existence at protein level was only available for 13 % of these proteins
301 (15 proteins out of 116), the remaining ones were either predicted as hypothetical proteins or inferred
302 from homology as reported in UniProtKB (supplementary material Table S1). In order to map the
303 secretion routes and SCL of these proteins experimentally identified, a secretomic analysis was
304 performed on the proteosurfaceome data set presently obtained (Figure 3 and supplementary material
305 Table S1). All-in-all, 69 % (80 out of 116) of the proteins identified were indeed predicted to localised
306 at the cell surface either as attached, integrated or loosely bound to the cytoplasmic membrane or cell
307 wall.

308 Searching for the presence of N-terminal SP, 31 proteins exhibited a SP, including 11 proteins
309 with a SP1, 12 with a SP2 and 8 with an uSP, which were therefore exported across the CM in a Sec-
310 dependent manner (supplementary material Table S1). Among the proteins exhibiting a SP1 and thus
311 cleaved by a signal peptidase of type I (SPase 1), 3 were predicted as iCM localised as they exhibited
312 several TMDs and thus corresponded to multi-spanning integral membrane protein of type 1
313 (msIMP1) inserted in a YidC-dependent manner. Five of the SP1-proteins were predicted with a SCL
314 at the CW, 2 cell-wall proteins (CWPs) were predicted to bind non-covalently to the CW as they
315 exhibited SH3-8 (also called GW) or LysM domains [13], while the 3 other CWPs harboured a C-
316 terminal LPXTG domain and were thus predicted as covalently anchored to the CW by sortases; two
317 of them are substrates to sortase A (SrtA) and one to SrtB. The 3 remaining SP1-proteins were
318 predicted as localised in the extracellular milieu (EM; GO:0005576) and thus corresponded to
319 exoproteins (EPs). The 12 proteins exhibiting a SP2 were predicted to be post-translationally
320 maturated by the lipoprotein diacylglyceryl transferase (Lgt) and then cleaved by a SPase 2 [15].
321 While these lipoproteins were primarily predicted as aCM localised, one of them also exhibited
322 several TMDs and was actually iCM localised, which additionally corresponded to a msIMP1.
323 Besides, 9 lipoproteins exhibited a glycine residue at position +2 of the SP cleaving site, and thus

324 could be further predicted as partly located in the EM [62]. The uSP plays the role of a signal anchor
325 to the CM and such proteins correspond to IMP2 inserted to the CM via YidC. While 6 IMP2 were
326 solely anchored to the CM by their uSP and corresponded to single-spanning IMP2 (ssIMP2), 2 IMP2
327 exhibited more than one TMD and corresponded to msIMP2. Among the 18 IMPs, 6 of them lacked
328 a SP, including 3 msIMP2, 2 ssIMP3 and one msIMP3, presumably translocated and inserted in a
329 YidC-only dependent-manner. Of note, all IMPs likely follow the Srp (signal recognition particle)
330 pathway involving a ribonucleoprotein complex with Ffh and its cognate membrane receptor FtsY
331 before joining Sec and/or YidC. No protein exhibiting a SP targeting the Tat (twin-arginine
332 translocation), ABC (ATP-binding cassette) protein exporter or Fpe pathway could be here identified.
333 Regarding the proteins devoid of a SP, one was predicted as subunit of cell surface appendage
334 (SCSA) and cell-surface exposed following export and assembly by the Fea to form the flagellum but
335 none could be identified as secreted *via* the Esx (ESAT-6 secretion system, also called Wss for
336 WXG100 secretion system) or trafficking through holins. While the remaining 78 proteins lacked an
337 obvious SP of any type and were primarily predicted as localised in the cytoplasm (GO:0005737),
338 91 % of these cytoproteins (CPs) were further predicted to have extracytoplasmic localisation. Such
339 extracytoplasmic cytoproteins (ECCPs) could be transported *via* unknown protein trafficking route,
340 referred as non-classical secretion (Ncs) [63,64]. Some of these ECCPs are catabolic enzymes known
341 to moonlight as adhesins at the bacterial cell-surface, such as the Gap and enolase (Eno) [42] or the
342 bifunctional aldehyde/alcohol dehydrogenase Lap (*Listeria* adhesion protein) [41], or are
343 moonlighting chaperones, e.g. GroEL and TufA (translation elongation factor Tu, also known as EF-
344 Tu) [42]. While SecA2-dependent secretion cannot be predicted by bioinformatic tools, literature
345 survey indicated that at least 4 proteins here identified actually follow this pathway, including proteins
346 (i) lacking a SP with Lap [40], (ii) with a SP1, *i.e.* CwhA (cell-wall hydrolase A, previously known
347 as Iap [invasion associated protein] or P60 [protein of 60 kDa]) [26,38], or (iii) with a SP2, namely
348 OppA1 (oligopeptide ABC transporter subunit A1) [38,65] and TcsA (CD4+ T-cell stimulating

349 antigen, formerly called Csa) [38,66]. In any case, all these proteins are predicted as cell surface
350 localised, some either associated to the CW or tethered to CM. Applying the secretome concept,
351 cognate transport systems and post-translocational maturation routes encoded in the genome of
352 *L. monocytogenes* EGDe could be attributed for each protein identified here above as resumed in
353 Figure 3.

354 **Inactivation of SecA2 induce major changes in protein abundance in the proteosurfaceome of**
355 ***L. monocytogenes* EGDe**

356 Following a label-free quantitative proteomic analysis, the relative protein abundance in the
357 proteosurfaceome of *L. monocytogenes wt* was compared to the Δ*secA2* mutant. A significant shift in
358 protein abundance was observed for 48 proteins out of the 116 proteins (41 %) identified here above
359 (Table 2 and supplementary material Table S1); proteins demonstrating significant differences in
360 their abundance were further referred as differential proteins. The large majority of differential
361 proteins (96 %) showed lower relative abundance upon SecA2 inactivation (Table 2). This
362 differential proteosurfaceome was constituted of 4 lipoproteins, 8 IMPs (including 2 ssIMP2, 2
363 ssIMP3, 1 msIMP1, 2 msIMP2 and 1 msIMP3), 1 CWP, 1 EP and 34 ECCPs (including 2 proteins
364 primarily predicted as CPs only). Regarding molecular functions and as indicated by functional
365 enrichment in the network, proteins associated to binding (GO: 0005488) represented the majority of
366 the differential proteins, *i.e.* 60 % (29 proteins out of 48) followed by transporter activity
367 (GO: 0005215) and catalytic activity (GO: 0016874), *i.e.* 20 % each (supplementary material
368 Table S1).

369 Network analysis indicated that the 48 proteins showing differential abundances had more
370 functional and/or physical interactions among themselves than what would be expected for a random
371 set of proteins of similar size (p-value 2.5×10^{-5}) and were thus at least partially biologically
372 connected (Figure 4). Eleven clusters were further highlighted by MCL clustering, including three
373 large clusters (> 5 proteins) and 7 interacting clusters. A strong cluster with some biochemical

374 evidences of interactions was related to peptide transport with components of ABC transporters, *i.e.*
375 OppA1, OppA2, OppD, OppF, AppA and GlnP. With interactions experimentally evidenced, another
376 strong cluster of proteins involved in protein biosynthesis was highlighted, especially with the
377 elongation factor TufA and FusA, and the ribosomal proteins RspB, RspE, RspC and RplD. This
378 latter cluster shows some connections with the last large cluster related to metabolic process, such as
379 nucleoside metabolism (Prs1, Prs2), amino acid catabolism (BfmBAB) or organic acid metabolism
380 (Ldh1, PycA, AckA). While some additional clusters (and proteins) were independent, *e.g.* related to
381 oxidoreductase activities (YjlD, YumB), transport/binding (MglA, TcsA), or to teichoic acids
382 glycosylation (RfbA, RfbB), other association networks showed some connections with these three
383 main clusters, *e.g.* related to tRNA aminoacylation (GlyRS, MetRS, AsnRS), fatty acid biosynthesis
384 (AccC, FabG), or cell division (MinD, MreB, FtsA). Besides its involvement in protein trafficking
385 and considering the modification of the cell morphology upon SecA2 inactivation, which result from
386 a septation defect and lead to cell elongation, the lower abundance of proteins related to cell envelope
387 biogenesis (RfbA, RfB, AccC, FabG, DltD) and cell division (MinD, MreB, FtsA, Ftsh, MurC), in
388 addition to translation and protein export (GlyRS, MetRS, AsnRS, TufA, FusA, Rph, RspB, RspC,
389 RplD, RpsE, AtpD) (Table 2 and Figure 4), appears quite relevant to the phenotypes associated to
390 *L. monocytogenes* Δ*secA2*.

391 Except for CwhA (Lmo0582), the other proteins previously reported as SecA2-dependent
392 were indeed present in lower abundance in *L. monocytogenes* Δ*secA2* versus *wt*, namely Lap
393 (Lmo1634), OppA1 (Lmo2196), and TcsA (Lmo1388) (Table 2). None of the differential proteins
394 had their presence completely abolished in the cell-surface fraction upon SecA2 inactivation but the
395 greatest differences in relative quantitative abundances were observed for Ldh1 and MurC (fold
396 change of -55 and -41, respectively, compared to *L. monocytogenes wt*) which are both primarily
397 predicted as cytoplasmic and lacking a SP (Table 2; supplementary material Table S1). Like the large
398 majority of differential ECCPs (94 %, *i.e.* 32 out of 34 proteins), these two ectopic CPs were predicted

399 to follow a Ncs pathway (supplementary material Table S1) and were thus here reported for the first
400 time to be secreted in a SecA2-dependent manner. While this subproteomic analysis revealed the
401 SecA2 dependence for the traffic of the differential ECCPs, it also underscores theses CPs have
402 multiple final SCL and might moonlight at the cell surface of *L. monocytogenes* as do the bifunctional
403 aldehyde/alcohol dehydrogenase Lap (Lmo1634) or the elongation factor TufA (Lmo2653), which
404 acts as adhesins when present at the bacterial cell surface [42]. Besides some ectopic CPs, some
405 differential LPs and IMPs participate to the bacterial cell surface properties of, *e.g.* AppA (Lmo0135,
406 also known as CtaP), which contribute to surface hydrophobicity, as well as listerial adhesion [36],
407 OppA (Lmo2196, Lmo2569), AtpD (Lmo2529) and FtsH (Lmo0220) associated with lipid rafts [67],
408 or DltD (Lmo0971) involved in D-alanylation of lipoteichoic acid polymers, which modulates the
409 bacterial surface charge [68].

410 **DISCUSSION**

411 Previous investigations on the influence of SecA2 on surface colonisation phenotypes in
412 *L. monocytogenes*, especially bacterial adhesion and biofilm formation [31], suggested the
413 inactivation of the SecA2-only protein export pathway could influence the listerial cell surface.
414 Besides cellular dimorphism, *L. monocytogenes* forms rough *vs* smooth colonies [27,29,38] where
415 modifications of surface charges and hydrophobicity were reported depending on the strains [69].
416 Characterisation of the cell surface properties upon SecA2 inactivation here indicated the degree of
417 hydrophilicity and Lewis acid-base properties were significantly affected. Modulation of these
418 physico-chemical properties would result from modifications in the composition of cell surface, *i.e.*
419 the surfaceome, which in CW-monoderm bacteria recovers the phospholipids at the CM,
420 peptidoglycan, (lipo)teichoic acids and wall polysaccharides at the CW, and different categories of
421 proteins present in the cell envelope [13]. Considering that the proteins are the primary substrates of
422 the SecA2-only export pathway, constitute the most functional part of the surfaceome, and can
423 contribute to the changes of cell surface properties upon SecA2 inactivation, the proteosurfaceome

424 was investigated further, although it cannot be excluded that collateral effects could affect the
425 composition in other constituents of the listerial cell envelope.

426 In fact, DltD associated with D-alanylation of lipoteichoic acids (LTAs) was lower abundant
427 in the proteosurfaceome of *L. monocytogenes* Δ*secA2* versus *wt*, which could in turn modulate the
428 degree of D-alanylation of LTAs and, consequently, the physico-chemical properties of the bacterial
429 cell surface [68,70]. Interestingly, the modification of the cell envelope components by the addition
430 of D-alanine onto LTAs tunes the virulence level of *L. monocytogenes*, adhesion to host cell and is a
431 mechanism that further allows protection against cationic antimicrobial peptides [71]. Similarly,
432 AccC and FabG associated to lipid metabolism, especially fatty acid biosynthesis, or RfbA and RfbB
433 associated to glycosylation of wall teichoic acids (WTAs), could modulate the composition of the
434 CM or CW [68]. Besides serotyping, modulation of glycosidic substituents of WTAs were evidenced
435 to influence the virulence level of *L. monocytogenes* and intestinal phase of listeriosis [68,72–74].
436 The multifunctional cysteine transport-associated protein AppA was shown to modulate bacterial
437 surface hydrophobicity and membrane permeability, as well as being an adhesin [36]. Interestingly,
438 the flotillin FloA was identified in the present investigation with no significant changes in abundance
439 but FtsH and OppA are known proteins to be associated with membrane microdomains corresponding
440 to bacterial lipid rafts [67]. Altogether these proteins could account for modification in cell surface
441 properties of *L. monocytogenes* upon SecA2 inactivation.

442 When present, the SecA2 pathway is often regarded as contributing to bacterial virulence
443 [22,26,75,76]. As already mentioned for AppA involved in vacuolar escape [36], OppA is the LP
444 component of an oligopeptide ABC transport system and is also required for the virulence of
445 *L. monocytogenes* as it is involved in intracellular survival, intracytoplasmic multiplication in
446 macrophages and phagosomal escape [65]. Upon gene deletion, which resulted in attenuated
447 virulence in mouse model, GlnP was also demonstrated to play a role in virulence by inducing
448 immune response during intracellular growth in macrophages [77,78]. While Sod [39] and FbpA [79]

449 could not be presently identified in the proteosurfaceome, Lap [40,41] and TcsA [66], together with
450 OppA, were previously described as SecA2-dependent virulence factors in *L. monocytogenes*. OppA
451 and TcsA were also early reported in lower amount at the listerial cell surface [27]. Interestingly,
452 OppA, together with ChiA and CwhA, was previously reported as not significantly affected by SecA
453 depletion [80], where it was suggested these proteins could use an alternative export system such as
454 SecA2. Besides chitin degradation [81–83], ChiA participates to *L. monocytogenes* virulence by
455 repressing inducible nitric oxide synthase expression (iNOS) and increasing the rate of survival in the
456 host [84–86]. Of note, the SecA2-dependent cell-wall hydrolase CwhA, together with MurA,
457 originally considered to be virulence factors must actually be considered as inducing this effect
458 collaterally [29,43]; in fact, septation defect upon loss of SecA2 expression results in mislocation of
459 some key cell-surface virulence factors, namely the InlA contributing to internalisation and ActA
460 involved in actin polymerisation. Considering the dysmorphism of *L. monocytogenes* Δ*secA2* cells,
461 the differential abundance of LPs and IMPs in the cell envelope could also be a collateral effect of
462 SecA2 inactivation leading to their suboptimal final SCL. For instance, overabundance of some LPs
463 in the supernatant of *L. monocytogenes* Δ*secA2* was suggested to result from the propensity of
464 lipoproteins exhibiting a G at position +2 of the cleavage site (as AppA, TcsA, OppA1) to be released
465 from the cell surface following proteolysis [62,87,88]; this variation in the distribution of some
466 proteins between the cell surface and extracellular milieu could explain differences in fold change
467 between the proteosurfaceome and exoproteome upon SecA2 inactivation [26,38]. Similarly, the
468 higher abundance of the LPXTG-protein SvpA (Lmo2185, also known as Hpb2 or P64) in the
469 proteosurfaceome or the exoproteome as previously observed could result from an imbalance between
470 the rates of LPXTG protein secretion and cell-wall biogenesis (coinciding with cell division) when
471 considering the mechanism of covalent anchoring to the CW by sortases [38,89].

472 All-in-all, it thus appears several differential proteins are involved in virulence and
473 pathogenicity of *L. monocytogenes*, as well as bacterial adhesion, including OppA and several

474 moonlighting ECCPs like Lap or the elongation factor Tu (TufA) [40–42]. As reported in some other
475 bacterial species, the pyruvate/2-oxoglutarate dehydrogenase complex subunit E1 (BfmAB) could be
476 involved in fibronectin binding [90] and the elongation factor G (FusA) in binding to mucin [91].
477 Interestingly, nearly all differential ECCPs were previously identified in the CW fraction of
478 *L. monocytogenes* [92], were thus predicted to follow a Ncs pathway and considered as novel
479 moonlighting protein candidates, including adhesins [93]. While the molecular mechanisms by which
480 SecA2 allows specific and selective export of proteins with or without a SP remains irresolute [76,94],
481 it is possible that some ECCPs are secreted by piggybacking, especially when considering proteins
482 known to interact physically like the ribosomal and elongation factors associating to secreted proteins
483 in the course of protein co-translational translocation for instance.

484 In the end, the dependence of a subset of proteins to SecA2 induced major changes in the
485 proteosurfaceome of *L. monocytogenes* with profound phenotypic implications on virulence and
486 pathogenicity, biotope colonisation, bacterial adhesion and biofilm formation [26,30,31,95,96]. By
487 modulating at once its physiology, the cell differentiation upon SecA2 inactivation participates to the
488 reversible switch between saprophytic commensal and infectious pathogenic bacteria [97]; as an
489 opportunistic pathogen, *L. monocytogenes* is an aetiologic agent effective in individuals with
490 impaired cell-mediated immunity [98–100] and, from its ubiquitous but opportunistic nature, it can
491 even be viewed as a pathobiont [101,102]. However, the regulatory mechanism at play in the SecA2-
492 dependent dimorphism of listerial cells and colonies remain unclear. While single base substitution
493 or insertion, leading to stop-codon frameshift and resulting in truncated non-functional SecA2, was
494 early indicated for some strains [27], no mutations in the CDS or promoter regions could be later
495 reported by some others [30,103]. Nonetheless, this phase variation appears dependent on
496 environmental conditions (pH, NaCl and nutrient concentrations) and would also rely on
497 compensatory mechanisms in the activity of components of the secretion system [30]. Lately, the
498 topological factor DivIVA was shown to influence the activity of SecA2-only export pathway [104].

A better understanding of the regulation of SecA2 inactivation in the morphotype conversion is undoubtedly the next frontier. This knowledge is a prerequisite before considering the tuning of the virulence level and the colonisation ability of *L. monocytogenes*, and gaining advance insights about its physiopathology and ecophysiology in relation to this peculiar secretion route.

503 **TABLES**

504 **Table 1: Contact angles, surface tension components and degree of hydrophobicity of *L. monocytogenes* EGDe *wt* and Δ*secA2* strains**

Bacterial strain	Contact angles [a]			Surface tension components [b]					ΔG_{1w1} [c]
	θ_W	θ_F	$\theta_{\alpha\text{-}B}$	γ_S^{LW}	γ_S^{+}	γ_S^{-}	γ_S^{AB}	γ_S^{T}	
L. monocytogenes EGDe	35.4 ±3.4	28.1 ±2.1	39.4 ±3.0	34.9	1.7	40.1	16.4	51.3	16.2 ±0.5
L. monocytogenes Δ*secA2*	28.8 ±2.4	25.9 ±2.7	38.3 ±2.1	35.4	1.5	46.4	16.6	52.0	23.7 ±0.4

505 [a] Contact angles are expressed in degree. θ_W: contact angle with water, θ_F: contact angle with formamide, $\theta_{\alpha\text{-}B}$: contact angle with α-

506 bromonaphthalene. Values given ± the standard deviation.

507 [b] γ_S^{LW}: apolar Lifshtz-van der Waals surface energy component, γ_S^{+}: electron acceptor surface energy component, γ_S^{-}: electron donator surface free

508 energy component, γ_S^{AB}: polar Lewis acid-base component, γ_S^{T}: total surface free energy.

509 [c] ΔG_{1w1}: degree of hydrophobicity expressed in mJ/m^2.

510 **Table 2: Proteosurfaceome of *L. monocytogenes* EGDe outlined for proteins presenting significant differences in their abundance between**

511 **Δ*secA2* and *wt* strains.**

Identifier	Name	Annotation [a]	Subcat [b]	SCL [c]	Fold [d]	*p*-value [e]	Predicted protein trafficking route [f]
Lipoproteins							
Lmo0135	AppA	ABC-type dipeptide transport system, substrate-binding protein family 5 component	LP	EM/CS/CM/aCM	-1.7	1.9×10^{-4}	Sec/SecA/Lgt/SPase2
Lmo1388	TcsA	CD4+ T-cell stimulating antigen	LP	EM/CS/CM/aCM	-1.3	3.2×10^{-2}	Sec/SecA2/Lgt/SPase2
Lmo2196	OppA1	Oligopeptide ABC transporter, periplasmic oligopeptide-binding protein	LP	EM/CS/CM/aCM	-1.7	3.7×10^{-4}	Sec/SecA2/Lgt/SPase2
Lmo2569	OppA2	ABC-type oligopeptide transport system, substrate-binding protein component	LP	CS/CM/aCM	-1.5	2.6×10^{-2}	Sec/SecA/Lgt/SPase2
Integral membrane proteins							
Lmo0661	AhpD	Carboxymuconolactone decarboxylase	ssIMP2	CS/CM/iCM	+1.8	4.8×10^{-2}	Ffh/FtsY/Sec/SecA/YidC
Lmo0971	DltD	D-alanine esterification of (lipo)teichoic acid protein	ssIMP2	CS/CM/iCM	-1.9	1.5×10^{-2}	Ffh/FtsY/Sec/SecA/YidC
Lmo1538	GlpK	Glycerol kinase	ssIMP3	CS/CM/iCM	-14.0	4.3×10^{-2}	Ffh/FtsY/YidC
Lmo1238	RpH	Ribonuclease PH, tRNA nucleotidyltransferase	ssIMP3	CS/CM/iCM	-2.2	1.8×10^{-2}	Ffh/FtsY/YidC
Lmo0847	GlnP	Glutamine ABC transporter, ABC-type amino acid transport system, permease component	msIMP1	CS/CM/iCM	-2.2	2.7×10^{-2}	Ffh/FtsY/Sec/SecA/YidC/SPase1
Lmo0098	MptD	Phosphotransferase system, mannose/fructose/sorbose family IID component	msIMP2	CS/CM/iCM	-2.8	2.5×10^{-2}	Ffh/FtsY/YidC
Lmo0220	FtsH	ATP-dependent zinc metalloprotease	msIMP2	CS/CM/iCM	-2.2	1.5×10^{-4}	Ffh/FtsY/Sec/SecA/YidC

Lmo2638	YjlD	NADH dehydrogenase FAD-containing subunit	msIMP3	CS/CM/iCM	-1.7	2.0×10^{-2}	Ffh/FtsY/YidC
Cell-wall proteins							
Lmo2185	SvpA	Surface virulence-associated protein A	LPXTG-CWP	CS/CW	+2.9	4.2×10^{-3}	Sec/SPase1/SrtB
Exoproteins							
Lmo1883	ChiA	Chitinase A	EP	EM	-10.3	1.8×10^{-2}	Sec/SecA/SPase1
Extracytoplasmic cytoproteins							
Lmo0177	MetRS	Methionyl-tRNA synthetase	ECCP	EM/CS/CY	-5.6	8.5×10^{-4}	Ncs
Lmo0199	Prs1	Phosphoribosyl pyrophosphate synthetase 1	ECCP	EM/CS/CY	-2.6	3.1×10^{-2}	Ncs
Lmo0210	Ldh1	L-lactate dehydrogenase 1	ECCP	EM/CS/CY	-55.1	5.0×10^{-3}	Ncs
Lmo0509	Prs2	Phosphoribosyl pyrophosphate synthetase 2	ECCP	EM/CS/CY	-11.6	8.9×10^{-6}	Ncs
Lmo0727	GlmS	D-fructose-6-phosphate amidotransferase	ECCP	EM/CS/CY	-7.5	2.6×10^{-2}	Ncs
Lmo1072	PycA	Pyruvate carboxylase	ECCP	EM/CS/CY	-2.5	1.1×10^{-3}	Ncs
Lmo1081	RfbA	Glucose-1-phosphate thymidylyltransferase	ECCP	EM/CS/CY	-2.6	1.7×10^{-2}	Ncs
Lmo1083	RfbB	dTDP-glucose 4,6-dehydratase	ECCP	EM/CS/CY	-4.2	3.5×10^{-5}	Ncs
Lmo1357	AccC	Acetyl-CoA carboxylase	ECCP	EM/CS/CY	-3.6	2.8×10^{-4}	Ncs
Lmo1373	BfmBAB	Pyruvate/2-oxoglutarate dehydrogenase complex subunit	ECCP	EM/CS/CY	-5.3	2.0×10^{-3}	Ncs
Lmo1398	RecA	Recombinase A	ECCP	EM/CS/CY	-6.5	1.0×10^{-5}	Ncs
Lmo1458	GlyRS	Glycyl-tRNA synthetase β subunit	ECCP	EM/CS/CY	-5.4	7.2×10^{-6}	Ncs
Lmo1548	MreB	Cell shape determining protein	ECCP	EM/CS/CY	-3.6	5.3×10^{-4}	Ncs
Lmo1581	AckA	Acetate kinase 1	ECCP	EM/CS/CY	-8.3	1.2×10^{-4}	Ncs
Lmo1605	MurC	UDP-N-acetylmuramate-L-alanine ligase	ECCP	EM/CS/CY	-41.1	1.8×10^{-4}	Ncs

Lmo1634	Lap	Bifunctional aldehyde/alcohol dehydrogenase, listerial adhesion protein	ECCP	EM/CS/CY	-3.4	4.1×10^{-4}	Sec/SecA2
Lmo1658	RpsB	30S ribosomal protein S2	ECCP	EM/CS/CY	-3.2	1.3×10^{-4}	Ncs
Lmo1807	FabG	3-oxoacyl-(acyl-carrier-protein) reductase	ECCP	EM/CS/CY	-2.2	1.4×10^{-2}	Ncs
Lmo1849	MntB	ABC-type Mn/Zn transport system, ATPase component, Manganese transport system ATP-binding protein	ECCP	EM/CS/CY	-6.3	3.0×10^{-3}	Ncs
Lmo1896	AsnRS	Asparagine-tRNA ligase	ECCP	EM/CS/CY	-2.0	7.8×10^{-3}	Ncs
Lmo2033	FtsA	Cell division protein	ECCP	EM/CS/CY	-8.1	4.8×10^{-2}	Ncs
Lmo2072	Rex	Redox-sensing transcriptional repressor	ECCP	EM/CS/CY	-12.6	2.5×10^{-5}	Ncs
Lmo2192	OppF	Oligopeptide transport ATP-binding protein	ECCP	EM/CS/CY	-3.8	3.0×10^{-5}	Ncs
Lmo2193	OppD	Oligopeptide transport ATP-binding protein	ECCP	EM/CS/CY	-3.6	1.5×10^{-4}	Ncs
Lmo2340	PsuG	Pseudouridine-5'-phosphate glycosidase (PsiMP glycosidase) (EC 4.2.1.70)	ECCP	EM/CS/CY	-1.9	2.1×10^{-2}	Ncs
Lmo2389	YumB	NAD-disulfide oxidoreductase	ECCP	EM/CS/CY	-27.7	8.0×10^{-3}	Ncs
Lmo2529	AtpD	F0F1 ATP synthase, subunit β	ECCP	EM/CS/CY	-3.4	2.6×10^{-4}	Ncs
Lmo2615	RpsE	30S ribosomal protein S5	ECCP	EM/CS/CY	-2.8	1.1×10^{-3}	Ncs
Lmo2626	RpsC	30S ribosomal protein S3	ECCP	EM/CS/CY	-1.7	3.6×10^{-2}	Ncs
Lmo2631	RplD	50S ribosomal protein L4	ECCP	EM/CS/CY	-4.9	8.2×10^{-3}	Ncs
Lmo2653	TufA	Elongation factor Tu (EF-Tu)	ECCP	EM/CS/CY	-2.0	3.6×10^{-2}	Ncs
Lmo2654	FusA	Translation elongation factor G (EF-G, EF2)	ECCP	EM/CS/CY	-2.3	1.3×10^{-2}	Ncs
Lmo1389	MglA	Galactose/methyl galactoside import ATP-binding protein	CP	CY	-2.3	3.6×10^{-2}	-

Lmo1544	MinD	Septum site-determining protein	CP	CY	-20.6	4.3×10^{-2}	-

[a] Compared to the original GenBank record, some annotations were corrected following proteogenomic analysis as described in the Material and Methods section and detailed in the supplementary material Table S1.

[b] Protein subcategory (Subcat) as primarily predicted following bioinformatic analysis as described in the Material and Methods section and detailed in the supplementary material Table S1. LP: lipoprotein; IMP: integral membrane protein; ssIMPx: single-spanning integral membrane protein of type x (x=2: type II; x=3: type III); msIMP: multi-spanning integral membrane protein of type x (x=1: type 1; x=2: type II; x=3: type III); LPXTG-CWP; cell-wall protein with a LPXTG motif; EP: exoprotein (extracellular protein); ECCP: extracytoplasmic cytoprotein; CP: cytoprotein (cytoplasmic protein).

[c] Predicted subcellular localisation (SCL) as primarily predicted following bioinformatic analysis as described in the Material and Methods section and detailed in the supplementary material Table S1. EM: extracellular milieu (GO:0005576); CS: cell surface (GO:0009986); CW: cell wall (GO:0005618); CM: cytoplasmic membrane (CM; GO:0005886); iCM: integral to the cytoplasmic membrane (GO:0005887); aCM: anchored to the cytoplasmic membrane (GO:00046658); CY: cytoplasm (GO:0005737).

[d] Fold change corresponds to the differential protein abundance in the Δ*secA2* mutant compared to the wild type (*wt*) strain, where -(x) means x-fold lower and +(x) means x-fold higher in *L. monocytogenes* Δ*secA2*.

[e] Difference in abundance was considered significant for *p*-values below 0.05. *q*-values are further provided in supplementary material Table S1.

[f] Protein trafficking routes as predicted by the secretomic analysis and literature survey as described in the Material and Methods section and detailed in the supplementary material Table S1. Ffh: protein subunit of SRP); FtsY: SRP receptor; Sec: Sec translocon; SecA: protein translocation ATPase forming the translocase together with the Sec translocon; SecA2: accessory protein translocation ATPase; Lgt: lipoprotein diacylglyceryl transferase; SPase x: signal peptidase of type x (x=1: type 1; x=2: type II), SrtB: sortase B; Ncs: non-classical secretion.

530 **FIGURES**

531 **Figure 1: Bacterial cell surface properties of *L. monocytogenes* EGDe *wt* and Δ*secA2* strains.**
532 Electrophoretic mobility by microelectrophoresis (A) and solvent affinity by MATS method (B), were
533 assayed as detailed in the Material and Methods section for *L. monocytogenes* EGDe *wt* (blue, dot)
534 and Δ*secA2* (red, square) strains. Inserts in part A indicate the distribution (%) of cells exhibiting
535 different global net surface charges (mobility expressed in µm/s/V/cm).

536 **Figure 2: Adhesion of *L. monocytogenes* EGDe *wt* and Δ*secA2* strains to different supports**.
537 Bacterial adhesion to stainless steel, glass and PET surfaces was observed by epifluorescent
538 microscopy (the scale bar corresponds to 50 µm) (A) and adhered bacteria were expressed as
539 cells/cm² for *L. monocytogenes* EGDe *wt* (blue) and Δ*secA2* (red) strains (B) as described in the
540 Material and Methods section.

541 **Figure 3: Secretome based analysis of the proteins identified in the proteosurfaceome of**
542 ***L. monocytogenes* EGDe *wt* and Δ*secA2*.** Schematic representation of the protein trafficking routes,
543 including components of the secretion pathways with cognate transport and post-translocational
544 maturation systems and non-classical secretion (Ncs) for the proteins identified in the
545 proteosurfaceome. The different predicted categories of proteins are depicted in red and the number
546 of proteins identified is reported for the total proteins (black), for proteins presenting (grey) or not
547 (white) significant differential abundance between *L. monocytogenes* EGDe *wt* and Δ*secA2*.
548 Components of the different protein transport and maturation systems were identified and reported
549 with protein identifier where export systems are indicated in blue, insertase in yellow, post-
550 translocational maturation pathway in green, and in grey the systems encoded in *L. monocytogenes*
551 EGDe but not used by the proteins presently identified. Arrows indicate the trafficking routes with
552 the number of identified proteins using them. Detailed secretomic analysis is provided in
553 supplementary material Table S1. Sec: Secretion (Sec) translocase; SecA: protein translocation
554 ATPase forming the Sec translocase together with the SecYEG translocon; SecA2: accessory protein

555 translocation ATPase; Lgt: lipoprotein diacylglyceryl transferase; SPase1: signal peptidase of type I;
556 SPase2: signal peptidase of type II; Fea: flagellum export apparatus; Tat: twin-arginine translocation;
557 Ape: ABC protein exporter; Fpe: frimbrillin-protein exporter; Esx (ESAT-6 secretion system);
558 SCSA: subunit of cell surface appendages; CWP: cell-wall protein; LP: lipoprotein; IMP: integral
559 membrane proteins; EP: exoprotein; ECCP: extracytoplasmic cytoprotein, CP: cytoprotein; EM:
560 extracellular milieu (GO:0005576); CS: cell surface (GO:0009986); CW: cell wall (GO:0009275);
561 CM: cytoplasmic membrane (CM; GO:0005886); CY: cytoplasm (GO:0005737).

562 **Figure 4: Protein-protein interaction network of differential proteins identified in the**
563 **proteosurfaceome of *L. monocytogenes* EGDe *wt* and Δ*secA2*.** Each network node (sphere)
564 represents a protein produced by a single protein-coding gene locus. Edges (connecting lines)
565 represent protein-protein associations, which are meant to be specific and meaningful, *i.e.* proteins
566 that jointly contribute to a shared function without necessarily meaning they are physically binding
567 one with another. Clusters represent coherent groups of proteins.

AUTHOR'S CONTRIBUTIONS

MP and MD conceptualised the overarching aims of the research study. IC, RO, MG, PT, JMH, NC, CC, JA, MNBF, MP and MD conceived and designed the experiments. IC, RO, MG, PT, JMH, NC and CC performed the experiments and data acquisition. IC, RO, MG, PT, JMH, NC, CC, MH, JA, MNBF, MP and MD analysed and interpreted the data. MP and MD had management as well as coordination responsibility for the execution of the research work. MP and MD contributed to the acquisition of the financial supports and resources leading to this publication. IC, RO, MG, PT, JMH, NC, CC, MH, JA, MNBF, MP and MD wrote the article, including drafting and revising critically the manuscript for important intellectual content. All authors have declared no competing interests.

ACKNOWLEDGEMENTS

This work was supported in part by INRAE ("Institut National de Recherche pour l'Agriculture, l'Alimentation et l'Environnement", previously called INRA, "Institut National de la Recherche Agronomique"), NCN ("Narodowe Centrum Nauki") National Science Centre Poland (n°2013/09/B/NZ6/00710), ANR ("Agence National de la Recherche") PathoFood project (n°ANR-17-CE21-0002), COST (European Cooperation in Science and Technology) Action FA1202 BacFoodNet, RMT ("Réseau Mixte Technologique") CHLEAN ("Conception Hygiénique des Lignes et Equipements et Amélioration de la Nettoyabilité pour une alimentation saine et sure") and France-Poland CampusFrance EGIDE PHC ("Programme Hubert Curien") POLONIUM 2013 (n°28298ZE).

SUPPLEMENTARY MATERIAL

Table S1. Total proteins identified in the proteosurfaceome of *L. monocytogenes* EGDe.

REFERENCES

[1] F. Allerberger, M. Wagner, Listeriosis: a resurgent foodborne infection, Clin Microbiol Infect. 16 (2010) 16–23. https://doi.org/10.1111/j.1469-0691.2009.03109.x.

[2] K. Dhama, K. Karthik, R. Tiwari, M.Z. Shabbir, S. Barbuddhe, S.V.S. Malik, R.K. Singh, Listeriosis in animals, its public health significance (food-borne zoonosis) and advances in diagnosis and control: a comprehensive review, Vet. Q. 35 (2015) 211–235. https://doi.org/10.1080/01652176.2015.1063023.

[3] S. Lomonaco, D. Nucera, V. Filipello, The evolution and epidemiology of Listeria monocytogenes in Europe and the United States, Infect. Genet. Evol. 35 (2015) 172–183. https://doi.org/10.1016/j.meegid.2015.08.008.

[4] A. Le Monnier, A. Leclercq, Listeria et listériose : des animaux d'élevage à nos assiettes [Listeria and Listeriosis: from farm to fork], Pathol. Biol. 57 (2009) 17–22. https://doi.org/10.1016/j.patbio.2008.07.026.

[5] W.F. Schlech, D. Acheson, Foodborne Listeriosis, Clin. Infect. Dis. 31 (2000) 770–775. https://doi.org/10.1086/314008.

[6] A.L. Vivant, D. Garmyn, P. Piveteau, Listeria monocytogenes, a down-to-earth pathogen, Front. Cell. Infect. Microbiol. 3 (2013). https://doi.org/10.3389/Fcimb.2013.00087.

[7] E. Giaouris, E. Heir, M. Hébraud, N. Chorianopoulos, S. Langsrud, T. Moretro, O. Habimana, M. Desvaux, S. Renier, G.J. Nychas, Attachment and biofilm formation by foodborne bacteria in meat processing environments: Causes, implications, role of bacterial interactions and control by alternative novel methods, Meat Sci. 97 (2014) 298–309. https://doi.org/10.1016/j.meatsci.2013.05.023.

[8] T. Møretrø, S. Langsrud, Listeria monocytogenes: biofilm formation and persistence in food-processing environments, Biofilms. 1 (2004) 107–121.

[9] E.P. da Silva, E.C.P. De Martinis, Current knowledge and perspectives on biofilm

formation: the case of Listeria monocytogenes, Appl. Microbiol. Biotechnol. 97 (2013) 957–968. https://doi.org/10.1007/s00253-012-4611-1.

[10] A. Colagiorgi, P. Di Ciccio, E. Zanardi, S. Ghidini, A. Ianieri, A Look inside the Listeria monocytogenes Biofilms Extracellular Matrix, Microorganisms. 4 (2016) 22. https://doi.org/10.3390/microorganisms4030022.

[11] M. Guilbaud, P. Piveteau, M. Desvaux, S. Brisse, R. Briandet, Exploring the Diversity of Listeria monocytogenes Biofilm Architecture by High-Throughput Confocal Laser Scanning Microscopy and the Predominance of the Honeycomb-Like Morphotype, Appl. Environ. Microbiol. 81 (2015) 1813–1819. https://doi.org/10.1128/AEM.03173-14.

[12] C. Chagnot, M.A. Zorgani, T. Astruc, M. Desvaux, Proteinaceous determinants of surface colonization in bacteria: bacterial adhesion and biofilm formation from a protein secretion perspective, Front Microbiol. 4 (2013) 303. https://doi.org/10.3389/fmicb.2013.00303.

[13] M. Desvaux, T. Candela, P. Serror, Surfaceome and Proteosurfaceome in Parietal Monoderm Bacteria: Focus on Protein Cell-Surface Display, Front Microbiol. (2018). https://doi.org/10.3389/fmicb.2018.00100.

[14] S. Renier, P. Micheau, R. Talon, M. Hébraud, M. Desvaux, Subcellular localization of extracytoplasmic proteins in monoderm bacteria: Rational secretomics-based strategy for genomic and proteomic analyses, PLoS ONE. 7 (2012) e42982. https://doi.org/10.1371/journal.pone.0042982.

[15] M. Desvaux, M. Hébraud, The protein secretion systems in Listeria: inside out bacterial virulence, FEMS Microbiol Rev. 30 (2006) 774–805.

[16] M. Desvaux, E. Dumas, I. Chafsey, C. Chambon, M. Hébraud, Comprehensive appraisal of the extracellular proteins from a monoderm bacterium: theoretical and empirical exoproteomes of Listeria monocytogenes EGD-e by secretomics, J Proteome Res. 9 (2010) 5076–5092. https://doi.org/10.1021/pr1003642.

[17] E. Dumas, M. Desvaux, C. Chambon, M. Hébraud, Insight into the core and variant

639 exoproteomes of Listeria monocytogenes species by comparative subproteomic analysis, Proteomics.
640 9 (2009) 3136–3155. https://doi.org/10.1002/pmic.200800765.
641 [18] E. Dumas, B. Meunier, J.L. Berdagué, C. Chambon, M. Desvaux, M. Hébraud,
642 Comparative analysis of extracellular and intracellular proteomes of Listeria monocytogenes strains
643 reveals a correlation between protein expression and serovar, Appl Env. Microbiol. 74 (2008) 7399–
644 7409. https://doi.org/10.1128/AEM.00594-08.
645 [19] M. Ashburner, C.A. Ball, J.A. Blake, D. Botstein, H. Butler, J.M. Cherry, A.P. Davis,
646 K. Dolinski, S.S. Dwight, J.T. Eppig, M.A. Harris, D.P. Hill, L. Issel-Tarver, A. Kasarskis, S. Lewis,
647 J.C. Matese, J.E. Richardson, M. Ringwald, G.M. Rubin, G. Sherlock, Gene Ontology: tool for the
648 unification of biology, Nat. Genet. 25 (2000) 25–29. https://doi.org/10.1038/75556.
649 [20] E. Vrontou, A. Economou, Structure and function of SecA, the preprotein translocase
650 nanomotor, Biochim. Biophys. Acta BBA - Mol. Cell Res. 1694 (2004) 67–80.
651 https://doi.org/10.1016/j.bbamcr.2004.06.003.
652 [21] A.J. Driessen, P. Fekkes, J.P. van der Wolk, The Sec system, Curr. Opin. Microbiol. 1
653 (1998) 216–222. https://doi.org/10.1016/S1369-5274(98)80014-3.
654 [22] M.E. Feltcher, M. Braunstein, Emerging themes in SecA2-mediated protein export,
655 Nat Rev Microbiol. 10 (2012) 779–789. https://doi.org/10.1038/nrmicro2874.
656 [23] N.W. Rigel, H.S. Gibbons, J.R. McCann, J.A. McDonough, S. Kurtz, M. Braunstein,
657 The accessory SecA2 system of *Mycobacteria* requires ATP binding and the canonical SecA1, J.
658 Biol. Chem. 284 (2009) 9927–9936. https://doi.org/10.1074/jbc.M900325200.
659 [24] M. Braunstein, A.M. Brown, S. Kurtz, W.R.J. Jacobs, Two nonredundant SecA
660 homologues function in Mycobacteria, J Bacteriol. 183 (2001) 6979–6990.
661 [25] M. Popowska, Analysis of the peptidoglycan hydrolases of Listeria monocytogenes:
662 multiple enzymes with multiple functions, Pol J Microbiol. 53 (2004) 29–34.
663 [26] L.L. Lenz, S. Mohammadi, A. Geissler, D.A. Portnoy, SecA2-dependent secretion of

664 autolytic enzymes promotes Listeria monocytogenes pathogenesis, Proc Natl Acad Sci U A. 100
665 (2003) 12432–12437.
666 [27] L.L. Lenz, D.A. Portnoy, Identification of a second Listeria secA gene associated with
667 protein secretion and the rough phenotype, Mol Microbiol. 45 (2002) 1043–1056.
668 [28] A. Vermassen, S. Leroy, R. Talon, C. Provot, M. Popowska, M. Desvaux, Cell Wall
669 Hydrolases in Bacteria: Insight on the Diversity of Cell Wall Amidases, Glycosidases and Peptidases
670 Toward Peptidoglycan, Front. Microbiol. 10 (2019). https://doi.org/10.3389/fmicb.2019.00331.
671 [29] S. Machata, T. Hain, M. Rohde, T. Chakraborty, Simultaneous deficiency of both
672 MurA and p60 proteins generates a rough phenotype in Listeria monocytogenes, J Bacteriol. 187
673 (2005) 8385–8394.
674 [30] I.R. Monk, G.M. Cook, B.C. Monk, P.J. Bremer, Morphotypic Conversion in Listeria
675 monocytogenes Biofilm Formation: Biological Significance of Rough Colony Isolates, Appl.
676 Environ. Microbiol. 70 (2004) 6686–6694. https://doi.org/10.1128/AEM.70.11.6686-6694.2004.
677 [31] S. Renier, C. Chagnot, J. Deschamps, N. Caccia, J. Szlavik, S.A. Joyce, M. Popowska,
678 C. Hill, S. Knøchel, R. Briandet, M. Hébraud, M. Desvaux, Inactivation of the SecA2 protein export
679 pathway in Listeria monocytogenes promotes cell aggregation, impacts biofilm architecture and
680 induces biofilm formation in environmental condition, Env. Microbiol. 16 (2014) 1176–1192.
681 https://doi.org/10.1111/1462-2920.12257.
682 [32] S. Pilgrim, A. Kolb-Maurer, I. Gentschev, W. Goebel, M. Kuhn, Deletion of the gene
683 encoding p60 in Listeria monocytogenes leads to abnormal cell division and loss of actin-based
684 motility, Infect Immun. 71 (2003) 3473–3484.
685 [33] E.S. Giotis, I.S. Blair, D.A. McDowell, Morphological changes in Listeria
686 monocytogenes subjected to sublethal alkaline stress, Int. J. Food Microbiol. 120 (2007) 250–258.
687 https://doi.org/10.1016/j.ijfoodmicro.2007.08.036.
688 [34] L.L. Isom, Z.S. Khambatta, J.L. Moluf, D.F. Akers, S.E. Martin, Filament Formation

689 in Listeria monocytogenes, J. Food Prot. 58 (1995) 1031–1033. https://doi.org/10.4315/0362-028X-
690 58.9.1031.
691 [35] N.J. Rowan, A.A.G. Candlish, A. Bubert, J.G. Anderson, K. Kramer, J. McLauchlin,
692 Virulent Rough Filaments of Listeria monocytogenes from Clinical and Food Samples Secreting
693 Wild-Type Levels of Cell-Free p60 Protein, J. Clin. Microbiol. 38 (2000) 2643–2648.
694 https://doi.org/10.1128/JCM.38.7.2643-2648.2000.
695 [36] B. Xayarath, H. Marquis, G.C. Port, N.E. Freitag, Listeria monocytogenes CtaP is a
696 multifunctional cysteine transport-associated protein required for bacterial pathogenesis, Mol.
697 Microbiol. 74 (2009) 956–973. https://doi.org/10.1111/j.1365-2958.2009.06910.x.
698 [37] S. Renier, M. Hébraud, M. Desvaux, Molecular biology of surface colonization by
699 Listeria monocytogenes: an additional facet of an opportunistic Gram-positive foodborne pathogen,
700 Env. Microbiol. 13 (2011) 835–850. https://doi.org/10.1111/j.1462-2920.2010.02378.x.
701 [38] S. Renier, C. Chambon, D. Viala, C. Chagnot, M. Hebraud, M. Desvaux,
702 Exoproteomic analysis of the SecA2-dependent secretion in Listeria monocytogenes EGD-e, J
703 Proteomics. 80C (2013) 183–195. https://doi.org/10.1016/j.jprot.2012.11.027.
704 [39] C. Archambaud, M.A. Nahori, J. Pizarro-Cerda, P. Cossart, O. Dussurget, Control of
705 Listeria superoxide dismutase by phosphorylation, J Biol Chem. 281 (2006) 31812–31822.
706 [40] K.M. Burkholder, K.-P. Kim, K.K. Mishra, S. Medina, B.-K. Hahm, H. Kim, A.K.
707 Bhunia, Expression of LAP, a SecA2-dependent secretory protein, is induced under anaerobic
708 environment, Microbes Infect. 11 (2009) 859–867. https://doi.org/10.1016/j.micinf.2009.05.006.
709 [41] B. Jagadeesan, O.K. Koo, K.-P. Kim, K.M. Burkholder, K.K. Mishra, A. Aroonnual,
710 A.K. Bhunia, LAP, an alcohol acetaldehyde dehydrogenase enzyme in *Listeria*, promotes bacterial
711 adhesion to enterocyte-like Caco-2 cells only in pathogenic species, Microbiology,. 156 (2010) 2782–
712 2795. https://doi.org/10.1099/mic.0.036509-0.
713 [42] J. Schaumburg, O. Diekmann, P. Hagendorff, S. Bergmann, M. Rohde, S.

714 Hammerschmidt, L. Jansch, J. Wehland, U. Karst, The cell wall subproteome of Listeria
715 monocytogenes, Proteomics. 4 (2004) 2991–3006.
716 [43] S. Pilgrim, A. Kolb-Mäurer, I. Gentschev, W. Goebel, M. Kuhn, Deletion of the gene
717 encoding p60 in *Listeria monocytogenes* leads to abnormal cell division and loss of actin-based
718 motility, Infect. Immun. 71 (2003) 3473–3484. https://doi.org/10.1128/IAI.71.6.3473-3484.2003.
719 [44] P. Glaser, L. Frangeul, C. Buchrieser, C. Rusniok, A. Amend, F. Baquero, P. Berche,
720 H. Bloecker, P. Brandt, T. Chakraborty, A. Charbit, F. Chetouani, E. Couvé, A. De Daruvar, P.
721 Dehoux, E. Domann, G. Dominguez-Bernal, E. Duchaud, L. Durant, O. Dussurget, K.D. Entian, H.
722 Fsihi, F. Garcia-Del Portillo, P. Garrido, L. Gautier, W. Goebel, N. Gomez-Lopez, T. Hain, J. Hauf,
723 D. Jackson, L.M. Jones, U. Kaerst, J. Kreft, M. Kuhn, F. Kunst, G. Kurapkat, E. Madueno, A.
724 Maitournam, J. Mata Vicente, E. Ng, H. Nedjari, G. Nordsiek, S. Novela, B. De Pablos, J.C. Perez-
725 Diaz, R. Purcell, B. Remmel, M. Rose, T. Schlueter, N. Simoes, A. Tierrez, J.A. Vazquez-Boland, H.
726 Voss, J. Wehland, P. Cossart, Comparative genomics of Listeria species, Science. 294 (2001) 849–
727 852.
728 [45] W.W. Wilson, M.M. Wade, S.C. Holman, F.R. Champlin, Status of methods for
729 assessing bacterial cell surface charge properties based on zeta potential measurements, J. Microbiol.
730 Methods. 43 (2001) 153–164. https://doi.org/10.1016/S0167-7012(00)00224-4.
731 [46] R. Oliveira, J. Azeredo, P. Teixeira, A.P. Fonseca, The role of hydrophobicity in
732 bacterial adhesion, in: Bioline, 2001. http://repositorium.sdum.uminho.pt/ (accessed June 9, 2020).
733 [47] T. Nakari-Setälä, J. Azeredo, M. Henriques, R. Oliveira, J. Teixeira, M. Linder, M.
734 Penttilä, Expression of a Fungal Hydrophobin in the Saccharomyces cerevisiae Cell Wall: Effect on
735 Cell Surface Properties and Immobilization, Appl. Environ. Microbiol. 68 (2002) 3385–3391.
736 https://doi.org/10.1128/AEM.68.7.3385-3391.2002.
737 [48] H.J. Busscher, A.H. Weerkamp, H.C. van der Mei, A.W. van Pelt, H.P. de Jong, J.
738 Arends, Measurement of the surface free energy of bacterial cell surfaces and its relevance for

739 adhesion, Appl Env. Microbiol. 48 (1984) 980–3.

740 [49] S. Silva, P. Teixeira, R. Oliveira, J. Azeredo, Adhesion to and Viability of Listeria
741 monocytogenes on Food Contact Surfaces, J. Food Prot. 71 (2008) 1379–1385.
742 https://doi.org/10.4315/0362-028X-71.7.1379.

743 [50] C.J. Van Oss, L. Ju, M.K. Chaudhury, R.J. Good, Estimation of the polar parameters
744 of the surface tension of liquids by contact angle measurements on gels, J. Colloid Interface Sci. 128
745 (1989) 313–319. https://doi.org/10.1016/0021-9797(89)90345-7.

746 [51] E.A. Vogler, Structure and reactivity of water at biomaterial surfaces, Adv. Colloid
747 Interface Sci. 74 (1998) 69–117. https://doi.org/10.1016/s0001-8686(97)00040-7.

748 [52] M.-N. Bellon-Fontaine, J. Rault, C.J. van Oss, Microbial adhesion to solvents: a novel
749 method to determine the electron-donor/electron-acceptor or Lewis acid-base properties of microbial
750 cells, Colloids Surf. B Biointerfaces. 7 (1996) 47–53. https://doi.org/10.1016/0927-7765(96)01272-
751 6.

752 [53] M. Guilbaud, J. Bruzaud, E. Bouffartigues, N. Orange, A. Guillot, A. Aubert-
753 Frambourg, V. Monnet, J.-M. Herry, S. Chevalier, M.-N. Bellon-Fontaine, Proteomic response of
754 *Pseudomonas aeruginosa* PAO1 adhering to solid surfaces, Front. Microbiol. 8 (2017).
755 https://doi.org/10.3389/fmicb.2017.01465.

756 [54] R. Monteiro, I. Chafsey, S. Leroy, C. Chambon, M. Hébraud, V. Livrelli, M. Pizza, A.
757 Pezzicoli, M. Desvaux, Differential biotin labelling of the cell envelope proteins in
758 lipopolysaccharidic diderm bacteria: Exploring the proteosurfaceome of Escherichia coli using sulfo-
759 NHS-SS-biotin and sulfo-NHS-PEG4-bismannose-SS-biotin, J. Proteomics. 181 (2018) 16–23.
760 https://doi.org/10.1016/j.jprot.2018.03.026.

761 [55] J. Esbelin, T. Santos, C. Ribière, M. Desvaux, D. Viala, C. Chambon, M. Hébraud,
762 Comparison of three methods for cell surface proteome extraction of Listeria monocytogenes
763 biofilms, OMICS J. Integr. Biol. 22 (2018) 779–787. https://doi.org/10.1089/omi.2018.0144.

764 [56] T. Santos, M. Hébraud, Extraction and Preparation of Listeria monocytogenes
765 Subproteomes for Mass Spectrometry Analysis, in: E.M. Fox, H. Bierne, B. Stessl (Eds.), List.
766 Monocytogenes Methods Protoc., Springer US, New York, NY, 2021: pp. 137–153.
767 https://doi.org/10.1007/978-1-0716-0982-8_11.
768 [57] N.L. Anderson, R. Esquer-Blasco, J.-P. Hofmann, N.G. Anderson, A two-dimensional
769 gel database of rat liver proteins useful in gene regulation and drug effects studies, Electrophoresis.
770 12 (1991) 907–913. https://doi.org/10.1002/elps.1150121110.
771 [58] R. Westermeier, Sensitive, Quantitative, and Fast Modifications for Coomassie Blue
772 Staining of Polyacrylamide Gels, Proteomics. 6 (2006) 61–64.
773 https://doi.org/10.1002/pmic.200690121.
774 [59] P.D. Thomas, M.J. Campbell, A. Kejariwal, H. Mi, B. Karlak, R. Daverman, K.
775 Diemer, A. Muruganujan, A. Narechania, PANTHER: A Library of Protein Families and Subfamilies
776 Indexed by Function, Genome Res. 13 (2003) 2129–2141. https://doi.org/10.1101/gr.772403.
777 [60] D. Szklarczyk, A. Franceschini, S. Wyder, K. Forslund, D. Heller, J. Huerta-Cepas,
778 M. Simonovic, A. Roth, A. Santos, K.P. Tsafou, M. Kuhn, P. Bork, L.J. Jensen, C. von Mering,
779 STRING v10: protein–protein interaction networks, integrated over the tree of life, Nucleic Acids
780 Res. 43 (2015) D447–D452. https://doi.org/10.1093/nar/gku1003.
781 [61] E. Karunakaran, J. Mukherjee, B. Ramalingam, C.A. Biggs, "Biofilmology": a
782 multidisciplinary review of the study of microbial biofilms, Appl. Microbiol. Biotechnol. 90 (2011)
783 1869–1881. https://doi.org/10.1007/s00253-011-3293-4.
784 [62] H. Tjalsma, J.M. van Dijl, Proteomics-based consensus prediction of protein retention
785 in a bacterial membrane, Proteomics. 5 (2005) 4472–4482.
786 [63] J.D. Bendtsen, L. Kiemer, A. Fausboll, S. Brunak, Non-classical protein secretion in
787 bacteria, BMC Microbiol. 5 (2005) 58.
788 [64] J.D. Bendtsen, K.G. Wooldridge, Chapter 10: Non-classical secretion. In: Bacterial

789 secreted proteins: secretory mechanisms and role in pathogenesis. Ed: Wooldridge K., Caister
790 Academic Press, Norwich, United Kingdom. pp. 226-235, in: 2009.
791 [65] E. Borezee, E. Pellegrini, P. Berche, OppA of Listeria monocytogenes, an
792 oligopeptide-binding protein required for bacterial growth at low temperature and involved in
793 intracellular survival, Infect Immun. 68 (2000) 7069–7077.
794 [66] S. Sanderson, D.J. Campbell, N. Shastri, Identification of a CD4+ T cell-stimulating
795 antigen of pathogenic bacteria by expression cloning, J Exp Med. 182 (1995) 1751–1757.
796 [67] M. Bramkamp, D. Lopez, Exploring the existence of lipid rafts in bacteria, Microbiol
797 Mol Biol Rev. 79 (2015) 81–100. https://doi.org/10.1128/MMBR.00036-14.
798 [68] F. Carvalho, S. Sousa, D. Cabanes, How Listeria monocytogenes organizes its surface
799 for virulence, Front. Cell. Infect. Microbiol. 4 (2014). https://doi.org/10.3389/fcimb.2014.00048.
800 [69] J.S. Dickson, G.R. Siragusa, Cell surface charge and initial attachment characteristics
801 of rough strains of Listeria monocytogenes, Lett. Appl. Microbiol. 19 (1994) 192–196.
802 https://doi.org/10.1111/j.1472-765X.1994.tb00941.x.
803 [70] D.A. Boyd, D.G. Cvitkovitch, A.S. Bleiweis, M.Y. Kiriukhin, D.V. Debabov, F.C.
804 Neuhaus, I.R. Hamilton, Defects in d-Alanyl-Lipoteichoic Acid Synthesis in Streptococcus mutans
805 Results in Acid Sensitivity, J. Bacteriol. 182 (2000) 6055–6065.
806 [71] E. Abachin, C. Poyart, E. Pellegrini, E. Milohanic, F. Fiedler, P. Berche, P. Trieu-
807 Cuot, Formation of D-alanyl-lipoteichoic acid is required for adhesion and virulence of Listeria
808 monocytogenes, Mol. Microbiol. 43 (2002) 1–14. https://doi.org/10.1046/j.1365-2958.2002.02723.x.
809 [72] N. Faith, S. Kathariou, Y. Cheng, N. Promadej, B.L. Neudeck, Q. Zhang, J.
810 Luchansky, C. Czuprynski, The Role of L. monocytogenes Serotype 4b gtcA in Gastrointestinal
811 Listeriosis in A/J Mice, Foodborne Pathog. Dis. 6 (2008) 39–48.
812 https://doi.org/10.1089/fpd.2008.0154.
813 [73] N. Autret, I. Dubail, P. Trieu-Cuot, P. Berche, A. Charbit, Identification of new genes

814 involved in the virulence of Listeria monocytogenes by signature-tagged transposon mutagenesis,
815 Infect Immun. 69 (2001) 2054–2065.
816 [74] E.T. Sumrall, A.P. Keller, Y. Shen, M.J. Loessner, Structure and function of Listeria
817 teichoic acids and their implications, Mol. Microbiol. 113 (2020) 627–637.
818 https://doi.org/10.1111/mmi.14472.
819 [75] B.A. Bensing, P.M. Sullam, An accessory sec locus of Streptococcus gordonii is
820 required for export of the surface protein GspB and for normal levels of binding to human platelets,
821 Mol Microbiol. 44 (2002) 1081–1094.
822 [76] B.A. Bensing, R. Seepersaud, Y.T. Yen, P.M. Sullam, Selective transport by SecA2:
823 An expanding family of customized motor proteins, Biochim. Biophys. Acta BBA - Mol. Cell Res.
824 1843 (2014) 1674–1686. https://doi.org/10.1016/j.bbamcr.2013.10.019.
825 [77] A. Bigot, C. Raynaud, I. Dubail, M. Dupuis, H. Hossain, T. Hain, T. Chakraborty, A.
826 2009 Charbit, lmo1273, a novel gene involved in Listeria monocytogenes virulence, Microbiology.
827 155 (2009) 891–902. https://doi.org/10.1099/mic.0.022277-0.
828 [78] T. Burg-Golani, Y. Pozniak, L. Rabinovich, N. Sigal, R. Nir Paz, A.A. Herskovits,
829 Membrane Chaperone SecDF Plays a Role in the Secretion of Listeria monocytogenes Major
830 Virulence Factors, J. Bacteriol. 195 (2013) 5262–5272. https://doi.org/10.1128/JB.00697-13.
831 [79] S. Dramsi, F. Bourdichon, D. Cabanes, M. Lecuit, H. Fsihi, P. Cossart, FbpA, a novel
832 multifunctional Listeria monocytogenes virulence factor, Mol Microbiol. 53 (2004) 639–649.
833 [80] S. Halbedel, S. Reiss, B. Hahn, D. Albrecht, G.K. Mannala, T. Chakraborty, T. Hain,
834 S. Engelmann, A. Flieger, A Systematic Proteomic Analysis of Listeria monocytogenes House-
835 keeping Protein Secretion Systems, Mol. Cell. Proteomics MCP. 13 (2014) 3063–3081.
836 https://doi.org/10.1074/mcp.M114.041327.
837 [81] J.J. Leisner, M.H. Larsen, R.L. Jorgensen, L. Brondsted, L.E. Thomsen, H. Ingmer,
838 Chitin hydrolysis by Listeria spp., including L. monocytogenes, Appl Env. Microbiol. 74 (2008)

839 3823–3830.

840 [82] D.K. Paspaliari, V.G. Kastbjerg, H. Ingmer, M. Popowska, M.H. Larsen, Chitinase
841 Expression in Listeria monocytogenes Is Influenced by lmo0327, Which Encodes an Internalin-Like
842 Protein, Appl. Environ. Microbiol. 83 (2017). https://doi.org/10.1128/AEM.01283-17.

843 [83] D.K. Paspaliari, J.S.M. Loose, M.H. Larsen, G. Vaaje-Kolstad, Listeria
844 monocytogenes has a functional chitinolytic system and an active lytic polysaccharide
845 monooxygenase, FEBS J. 282 (2015) 921–936. https://doi.org/10.1111/febs.13191.

846 [84] M.H. Larsen, J.J. Leisner, H. Ingmer, The Chitinolytic Activity of Listeria
847 monocytogenes EGD Is Regulated by Carbohydrates but Also by the Virulence Regulator PrfA, Appl.
848 Environ. Microbiol. 76 (2010) 6470–6476. https://doi.org/10.1128/AEM.00297-10.

849 [85] S. Chaudhuri, B.N. Gantner, R.D. Ye, N.P. Cianciotto, N.E. Freitag, The Listeria
850 monocytogenes ChiA Chitinase Enhances Virulence through Suppression of Host Innate Immunity,
851 MBio. 4 (2013). https://doi.org/10.1128/mBio.00617-12.

852 [86] S. Chaudhuri, J.C. Bruno, F. Alonzo, B. Xayarath, N.P. Cianciotto, N.E. Freitag,
853 Contribution of Chitinases to Listeria monocytogenes Pathogenesis, Appl. Environ. Microbiol. 76
854 (2010) 7302–7305. https://doi.org/10.1128/AEM.01338-10.

855 [87] H. Antelmann, H. Tjalsma, B. Voigt, S. Ohlmeier, S. Bron, J.M. van Dijl, M. Hecker,
856 A proteomic view on genome-based signal peptide predictions, Genome Res. 11 (2001) 1484–1502.

857 [88] L. Westers, H. Westers, G. Zanen, H. Antelmann, M. Hecker, D. Noone, K.M. Devine,
858 J.M. van Dijl, W.J. Quax, Genetic or chemical protease inhibition causes significant changes in the
859 Bacillus subtilis exoproteome, Proteomics. 8 (2008) 2704–2713.
860 https://doi.org/10.1002/pmic.200800009.

861 [89] H. Ton-That, L.A. Marraffini, O. Schneewind, Protein sorting to the cell wall envelope
862 of Gram-positive bacteria, Biochim Biophys Acta-Mol Cell Res. 1694 (2004) 269–278.

863 [90] S.F. Dallo, T.R. Kannan, M.W. Blaylock, J.B. Baseman, Elongation factor Tu and E1

beta subunit of pyruvate dehydrogenase complex act as fibronectin binding proteins in Mycoplasma pneumoniae, Mol. Microbiol. 46 (2002) 1041–1051. https://doi.org/10.1046/j.1365-2958.2002.03207.x.

[91] M. Kesimer, N. Kiliç, R. Mehrotra, D.J. Thornton, J.K. Sheehan, Identification of salivary mucin MUC7 binding proteins from Streptococcus gordonii, BMC Microbiol. 9 (2009) 163. https://doi.org/10.1186/1471-2180-9-163.

[92] F. Garcia-Del Portillo, E. Calvo, V. D'Orazio, M.G. Pucciarelli, Association of ActA to the peptidoglycan revealed by cell wall proteomics of intracellular Listeria monocytogenes, J Biol Chem. (2011). https://doi.org/10.1074/jbc.M111.230441.

[93] W. Wang, C.J. Jeffery, An analysis of surface proteomics results reveals novel candidates for intracellular/surface moonlighting proteins in bacteria, Mol. Biosyst. 12 (2016) 1420–1431. https://doi.org/10.1039/C5MB00550G.

[94] B.K. Miller, K.E. Zulauf, M. Braunstein, The Sec Pathways and Exportomes of Mycobacterium tuberculosis, in: Tuberc. Tuber. Bacillus, John Wiley & Sons, Ltd, 2017: pp. 607–625. https://doi.org/10.1128/9781555819569.ch28.

[95] E. Muraille, E. Narni-Mancinelli, P. Gounon, D. Bassand, N. Glaichenhaus, L.L. Lenz, G. Lauvau, Cytosolic expression of SecA2 is a prerequisite for long-term protective immunity, Cell. Microbiol. 9 (2007) 1445–1454. https://doi.org/10.1111/j.1462-5822.2007.00883.x.

[96] M. Rahmoun, M. Gros, L. Campisi, D. Bassand, A. Lazzari, C. Massiera, E. Narni-Mancinelli, P. Gounon, G. Lauvau, Priming of Protective Anti-Listeria monocytogenes Memory CD8+ T Cells Requires a Functional SecA2 Secretion System ▿, Infect. Immun. 79 (2011) 2396–2403. https://doi.org/10.1128/IAI.00020-11.

[97] M.J. Gray, N.E. Freitag, K.J. Boor, How the bacterial pathogen Listeria monocytogenes mediates the switch from environmental Dr. Jekyll to pathogenic Mr. Hyde, Infect Immun. 74 (2006) 2505–2512.

[98] M. Schuppler, M.J. Loessner, The Opportunistic Pathogen Listeria monocytogenes: Pathogenicity and Interaction with the Mucosal Immune System, Int. J. Inflamm. 2010 (2010) e704321. https://doi.org/10.4061/2010/704321.

[99] L.T. Matereke, A.I. Okoh, Listeria monocytogenes Virulence, Antimicrobial Resistance and Environmental Persistence: A Review, Pathogens. 9 (2020) 528. https://doi.org/10.3390/pathogens9070528.

[100] N. Rolhion, P. Cossart, How the study of Listeria monocytogenes has led to new concepts in biology, Future Microbiol. 12 (2017) 621–638. https://doi.org/10.2217/fmb-2016-0221.

[101] L. Jochum, B. Stecher, Label or Concept – What Is a Pathobiont?, Trends Microbiol. 28 (2020) 789–792. https://doi.org/10.1016/j.tim.2020.04.011.

[102] N. Kamada, G.Y. Chen, N. Inohara, G. Núñez, Control of pathogens and pathobionts by the gut microbiota, Nat. Immunol. 14 (2013) 685–690. https://doi.org/10.1038/ni.2608.

[103] J. Durack, T.P. Burke, D.A. Portnoy, A prl Mutation in SecY Suppresses Secretion and Virulence Defects of Listeria monocytogenes secA2 Mutants, J. Bacteriol. 197 (2015) 932–942. https://doi.org/10.1128/JB.02284-14.

[104] S. Halbedel, B. Hahn, R.A. Daniel, A. Flieger, DivIVA affects secretion of virulence-related autolysins in Listeria monocytogenes, Mol. Microbiol. 83 (2012) 821–839. https://doi.org/10.1111/j.1365-2958.2012.07969.x.

Figure 1

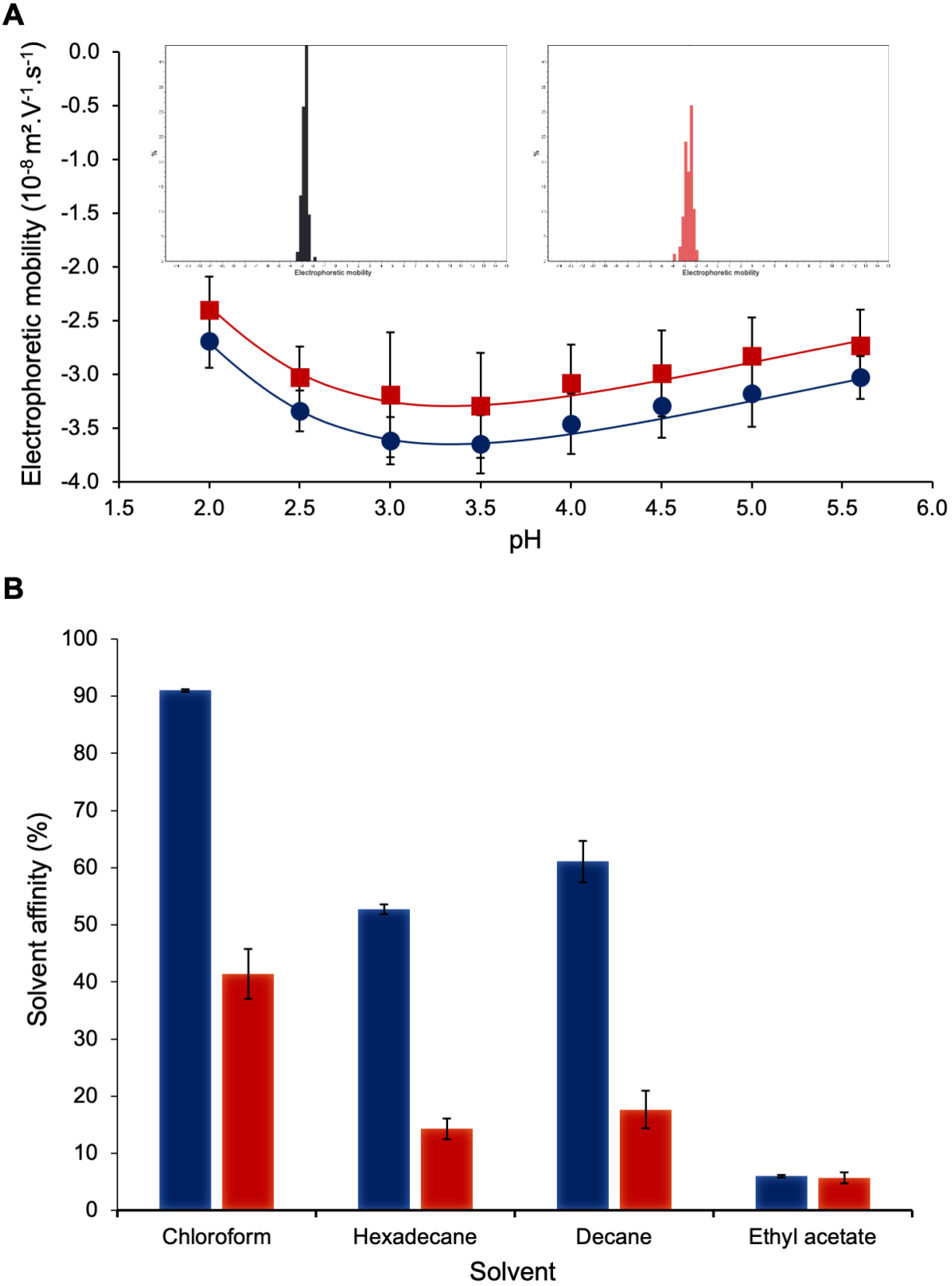
A
Electrophoretic mobility (10^{-8} m².V^{-1}.s^{-1})
0.0
-0.5
-1.0
-1.5
-2.0
-2.5
-3.0
-3.5
-4.0
1.5
2.0
2.5
3.0
3.5
4.0
4.5
5.0
5.5
6.0
pH
Electrophoretic mobility
Electrophoretic mobility
B
Solvent affinity (%)
100
90
80
70
60
50
40
30
20
10
0
Chloroform
Hexadecane
Decane
Ethyl acetate
Solvent

Figure 2

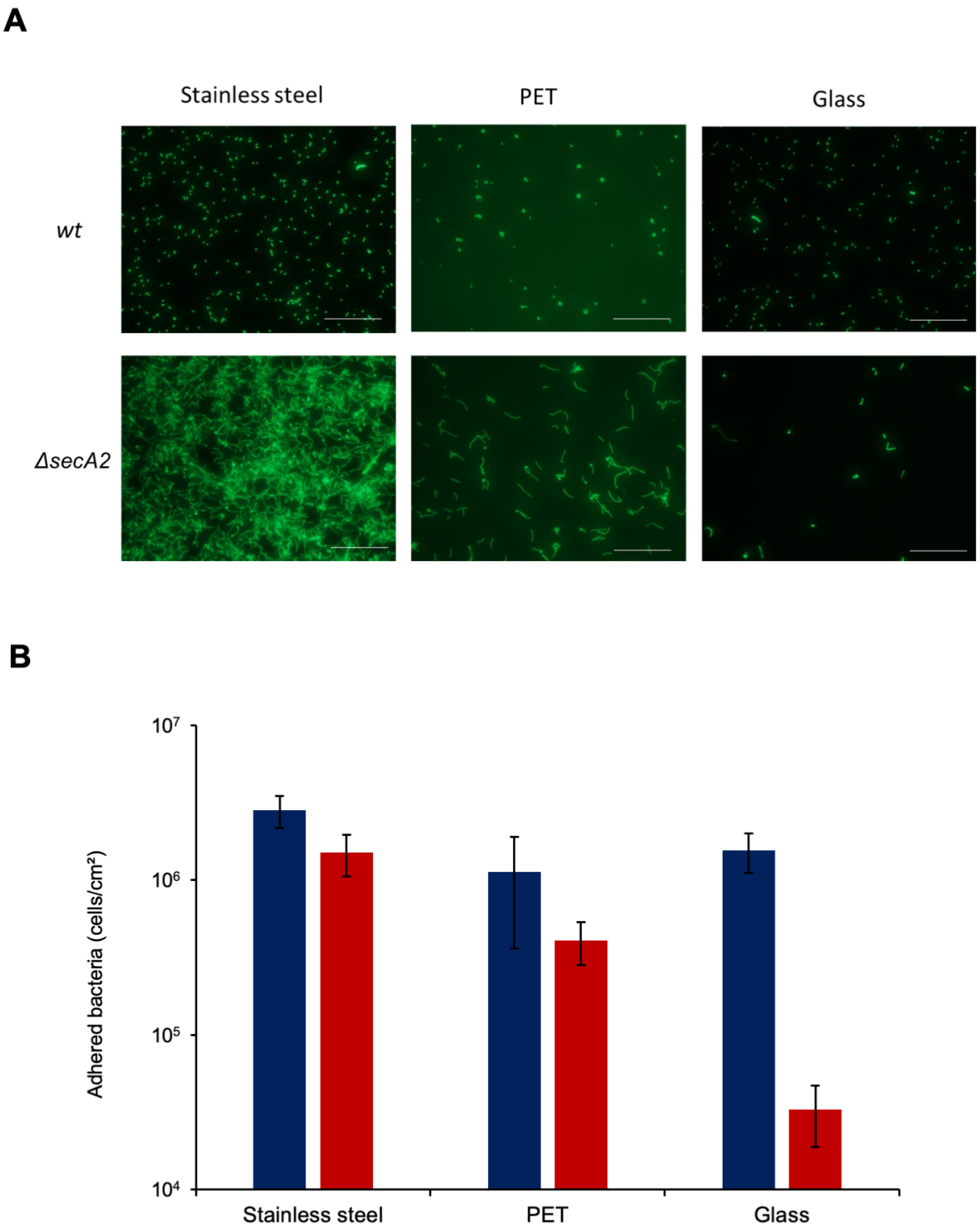
A
Stainless steel
PET
Glass
wt
ΔsecA2
B
Adhered bacteria (cells/cm²)
10⁷
10⁶
10⁵
10⁴
Stainless steel
PET
Glass

Figure 3

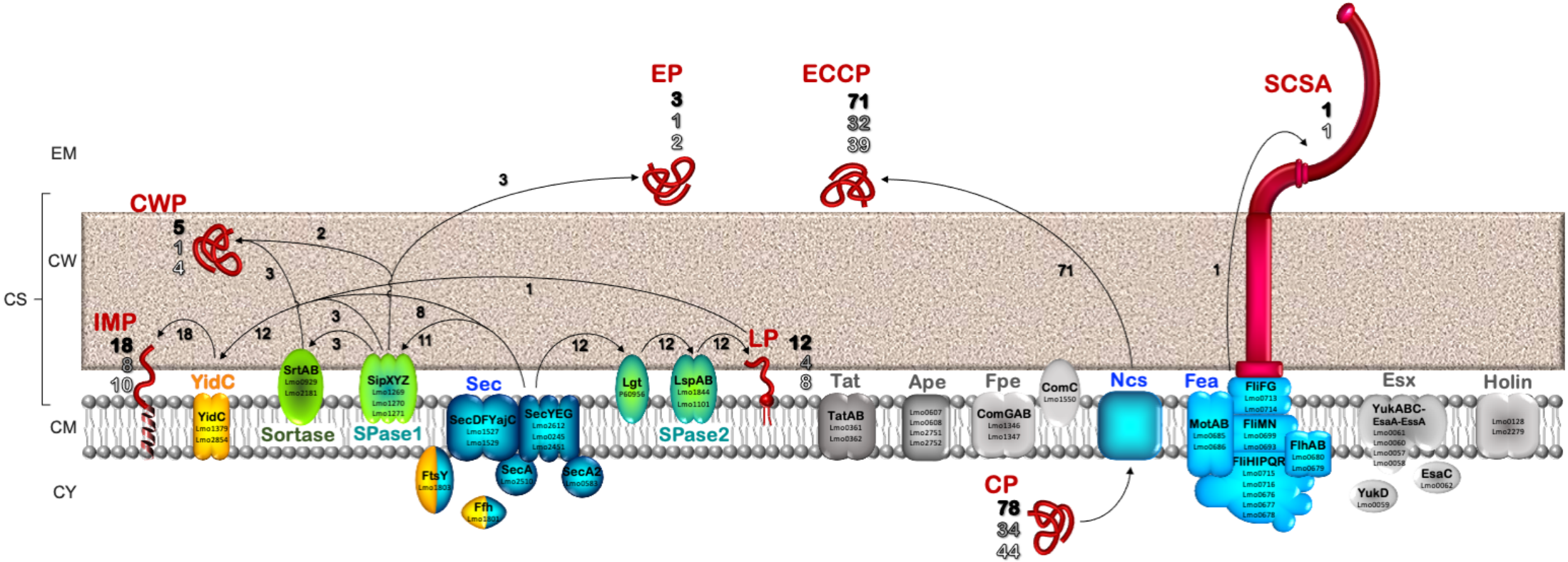
EM
CS
CW
CM
CY
CWP
5
1
4
EP
3
1
2
ECCP
71
32
39
SCSA
1
1
IMP
18
8
10
LP
12
4
8
CP
78
34
44
YidC
Sortase
SPase1
Sec
SPase2
Tat
Ape
Fpe
Ncs
Fea
Esx
Holin
SrtAB
SipXYZ
SecDFYajC
SecYEG
Lgt
LspAB
TatAB
ComGAB
ComC
MotAB
FliFG
FliMN
FliHIPQR
FlhAB
YukABC-EsaA-EssA
EsaC
YukD
FtsY
Ffh
SecA
SecA2

Figure 4

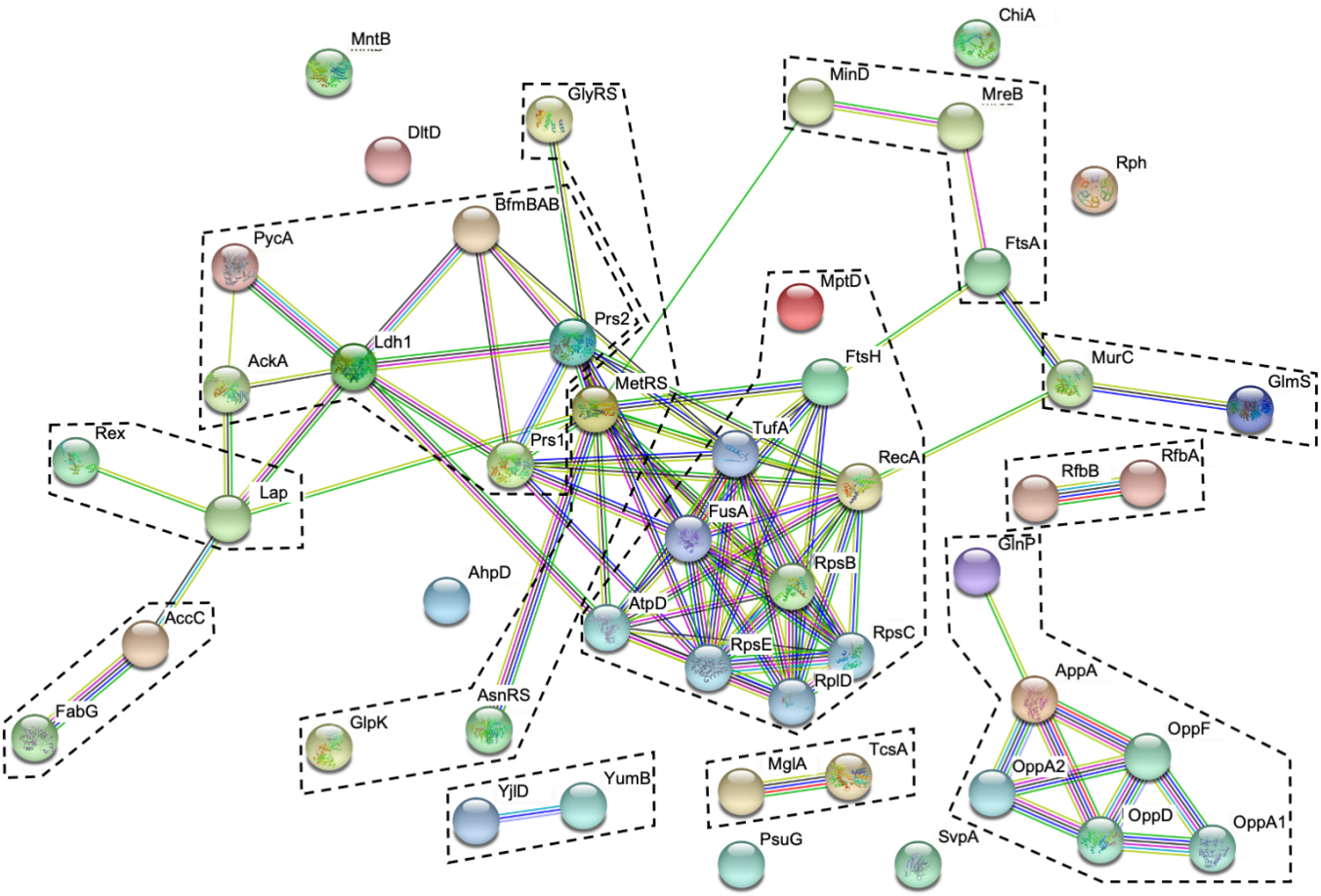

Node Content

empty nodes:
protein of unknown 3D structure

filled nodes:
some 3D structure is known or predicted

Node Color

colored nodes:
query proteins and first shell of interactors

white nodes:
second shell of interactors

Cluster

MCL clustering

Known Interactions

from curated databases

experimentally determined

Predicted Interactions

gene neighborhood

gene fusion

gene co-occurrence

Others

text mining

co-expression

protein similarity